JACS
JOURNAL OF THE AMERICAN CHEMICAL SOCIETY
pubs.acs.org/JACS

Article

π-Bonding of Group 11 Metals to a Tantalum Alkylidyne Alkyl Complex Promotes Unusual Tautomerism to Bis-alkylidene and CO_2 to Ketenyl Transformation

Abdelhak Lachguar, Iker Del Rosal, Laurent Maron, Erwann Jeanneau, Laurent Veyre, Chloé Thieuleux, and Clément Camp*

Cite This: J. Am. Chem. Soc. 2024, 146, 18306−18319

Read Online

ACCESS | Metrics & More | Article Recommendations | Supporting Information

ABSTRACT: A salt metathesis synthetic strategy is used to access rare tantalum/coinage metal (Cu, Ag, Au) heterobimetallic complexes. Specifically, complex $[Li(THF)_2][Ta(C^tBu)(CH_2{}^tBu)_3]$, **1**, reacts with (IPr)MCl (M = Cu, Ag, Au, IPr = 1,3-bis(2,6-diisopropylphenyl)imidazol-2-ylidene) to afford the alkylidyne-bridged species $[Ta(CH_2{}^tBu)_3(\mu\text{-}C^tBu)M(IPr)]$ **2-M**. Interestingly, π-bonding of group 11 metals to the Ta—C moiety promotes a rare alkylidyne alkyl to bis-alkylidene tautomerism, in which compounds **2-M** are in equilibrium with $[Ta(CH^tBu)(CH_2{}^tBu)_2(\mu\text{-}CH^tBu)M(IPr)]$ **3-M**. This equilibrium was studied in detail using NMR spectroscopy and computational studies. This reveals that the equilibrium position is strongly dependent on the nature of the coinage metal going down the group 11 triad, thus offering a new valuable avenue for controlling this phenomenon. Furthermore, we show that these uncommon bimetallic couples could open attractive opportunities for synergistic reactivity. We notably report an uncommon deoxygenative carbyne transfer to CO_2 resulting in rare examples of coinage metal ketenyl species, (^{t}BuCCO)M(IPr), **4-M** (M = Cu, Ag, Au). In the case of the Ta/Li analogue **1**, the bis(alkylidene) tautomer is not detected, and the reaction with CO_2 does not cleanly yield ketenyl species, which highlights the pivotal role played by the coinage metal partner in controlling these unconventional reactions.

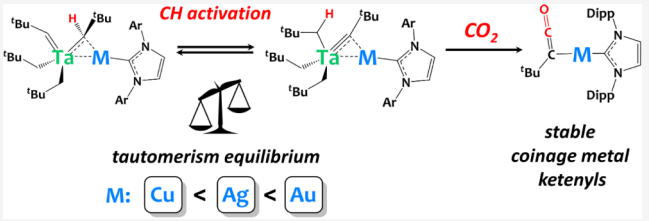

INTRODUCTION

The π-activation of unsaturated hydrocarbons, such as alkenes, dienes, alkynes, or allenes, via coinage metals is well-established[1−17] and led to numerous methodologies and applications, especially in organic chemistry and catalysis.[18−33] Coinage metals are also known to efficiently coordinate to a number of heteroelement-based π-systems,[34−47] yet practical applications of the latter still remain limited. Despite the interest of metal−carbon triple bonds in organometallic chemistry,[48−51] the activation of M—C motifs via external d-block metal centers is still in its infancy. This is exemplified by the limited advancements observed in the context of tantalum alkylidynes, primarily restricted to their interaction with zinc cations to the best of our knowledge.[52−55] Pfeffer and coworkers reported for instance an alkylidyne-bridged Ta/Zn species, which, in the presence of tmeda (tmeda = *N*,*N*,*N*′,*N*′-tetramethylethylenediamine), triggers intramolecular C−H bond activation (Scheme 1-top).[53] The same group also described a Pd-bound Ta alkylidene alkyl complex which, upon treatment with pyridine, leads to an unstable compound tentatively assigned to a Pd-coordinated tantalum alkylidyne (Scheme 1-bottom), but the latter could not be isolated.[56] These pioneering examples suggest that external metal reagents may serve as effective tools for controlling the reactivity of Ta alkylidyne moieties, offering the possibility of promoting atypical bimetallic C−H activations.[57] Yet to date coordination of transition metals to Ta—C moieties has not been exploited to trigger unusual reactivity.

Scheme 1. Literature Precedents for Tantalum Alkylidyne Reactivity with d-Block Metals

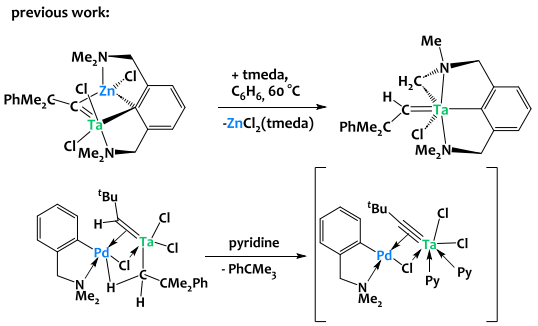

Received: February 12, 2024
Revised: April 26, 2024
Accepted: April 29, 2024
Published: June 27, 2024

Given the unique advantage of coinage metals for π-bonding to substrates, our interest was thus sparked in examining their interaction with Ta alkylidynes. This exploration not only has the potential to fine-tune the reactivity of the latter but could also open up a promising avenue for initiating carbyne transfer reactions. This is particularly noteworthy since the stabilization of coinage metal carbynes is extremely challenging,[58,59] despite their high interest and potential applications in organic chemistry and catalysis.

In this study, we illustrate that the tantalum alkylidyne moiety can efficiently bind coinage metal centers, leading to novel, well-defined, heterobimetallic compounds and triggering unusual reactivity. Specifically, we document an unusual deoxygenative carbyne transfer to CO_2, resulting in rare examples of coinage metal ketenyl M-C(*t*Bu)=C=O species (M = Cu, Ag, Au). The synthesis of ketenyls has received a notable surge in interest among organic and organometallic chemists in the past years,[60−66] but these are typically prepared from CO rather than CO_2. Cu(I) and Ag(I) ketenyl species were also proposed and debated as pivotal intermediates within catalytic cycles, for instance in the Kinugasa reaction, but had remained elusive and never isolated.[33,67−70] The bimetallic reactivity reported here could therefore open up new perspectives in carbyne transfer chemistry or catalysis.

RESULTS AND DISCUSSION

As part of our work in the preparation of tantalum-based early/late heterobimetallic complexes,[71−75] we contemplated the use of the *ate*-complex [Li(THF)$_2$][Ta(C*t*Bu)(CH$_2$*t*Bu)$_3$], **1**,[52] as an entry point *via* salt metathesis.[76−78] We determined the solid-state structure of **1** by single crystal X-ray diffraction (Figure 1), intending to establish a reference point for comparing metrical parameters with other compounds discussed in this study (Table 1).

The reaction between **1** and (IPr)CuCl affords the heterobimetallic complex [Ta(CH$_2$*t*Bu)$_3$(μ-C*t*Bu)Cu(IPr)], **2-Cu** (Scheme 2), which is isolated in excellent yield (93%). Compound **2-Cu** is diamagnetic. The ^{1}H NMR spectrum of **2-Cu** indicates that the three CH$_2$*t*Bu groups are equivalent in solution, resulting in two signals at 0.68 and 1.28 ppm, for the CH$_2$ and *t*Bu moieties, respectively. The analysis of the ^{13}C{^{1}H}-NMR spectrum of **2-Cu** reveals a distinct characteristic resonance at 286.52 ppm for the Ta—C alkylidyne moiety,[54,79] akin to complex **1** (281.77 ppm). The C_{NHC} carbene signal is observed at 185.57 ppm, which is consistent with literature data for (IPr)Cu(I) species.[80]

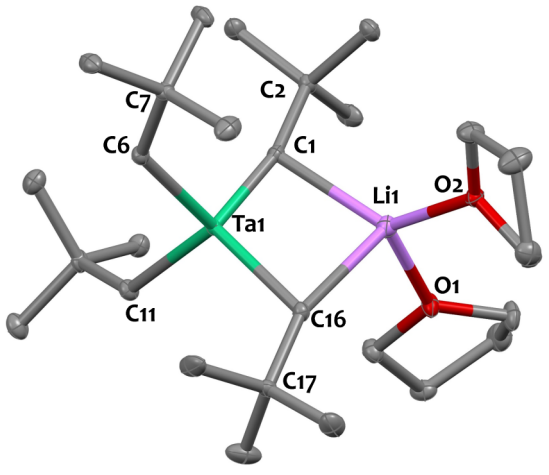

Figure 1. Solid state structure of **1**. Ellipsoids are represented with 30% probability. Hydrogen atoms have been omitted for clarity. Selected distances (Å) and angles (deg): Ta1−Li1 2.872(5), Ta1−C1 1.838(3), Ta1−C6 2.170(3), Ta1−C11 2.177(3), Ta1−C16 2.220(3), Li1−C1 2.223(6), Li1−C16 2.468 (6), Ta1−C1−C2 166.4(2), Ta1−C6−C7 131.2(2), Ta1−C16−C17 118.9(2).

The solid-state structure of **2-Cu**, determined by XRD, is shown in Figure 2 (top) and confirms the side-on coordination of the alkylidyne to the cationic Cu(NHC)$^+$ fragment. The Ta−C1 bond length (1.844(2) Å) in **2-Cu** is similar to that in **1** (1.838(3) Å) and that in the monometallic terminal alkylidyne complex Ta(CPh)(Cp*)$_2$(PMe$_3$) (1.849(8) Å).[81] This distance is significantly shorter than that typically found in ditantalum μ-alkylidyne species [1.93−1.99 Å][82] or tantalum neopentylidene complexes [1.90−2.03 Å].[56,71,72,74,83−85] This suggests that the Ta1−C1 bond has a significant triple bond character, as represented in the extreme resonance form in Scheme 2-right. Similar distances are found in related tantalum−zinc μ-alkylidyne species [1.79−1.86 Å].[53−55] The negligible deviation of C2 from the Ta1−C1−Cu1 plane (0.03(2) Å) is consistent with a pseudosp hybridized C1 center. The angle between the Ta1−C1 centroid, Cu1 and C21 from the NHC ligand (174.0(2)°) is close to linearity, a typical coordination geometry around Cu(I) centers. The Cu1−C21 distance (1.919(2) Å) is in agreement with literature data for copper(I)-NHC heterobimetallic complexes,[80,86] and the NHC carbon, C21, lies almost exactly in the Ta1−C1−Cu1 plane (mean deviation: 0.11(1) Å).

Molecular compounds associating Ta and Cu are extremely rare in the literature,[87−90] and to our knowledge, there is no structurally characterized tantalum/copper molecular complex featuring an unsupported metal−metal interaction (i.e., without bridging ligands) reported to date. A search in the CCDC database for Ta−Cu species, where the two metal centers are separated by 2.7 Å or less revealed only one recent study from Buss and Maiola, who reported hydride-bridged species, in which the Ta−Cu distances span the range [2.61−2.90 Å].[90] The Ta−Cu distance in **2-Cu** (2.7018(8) Å) is falling in this range, which is in between the sum of the respective metallic radii (Ta: 1.343 Å; Cu: 1.173 Å; sum = 2.516 Å)[91] and covalent radii (Ta: 1.70 Å; Cu: 1.32 Å; sum = 3.02 Å).[92] This provides a potential avenue for metal−metal interactions.

The silver and gold analogues, **2-Ag** and **2-Au**, were synthesized in excellent yields (92% and 89%, respectively) from the analogous reaction between **1** and (IPr)MCl (M = Ag, Au). In all cases, the NMR spectra were consistent with a single neopentyl and IPr environment, implying free rotation at room temperature on the NMR time scale.

The solid-state structures for **2-Ag** and **2-Au** are reproduced in Figure 2. Both compounds feature similar geometry, with the C2 and C21 carbons lying in the same plane than the Ta1−C1−M1 (M = Ag or Au) core. The Ta1−C1 distance is elongated from 1.844(2) Å in **2-Cu** to 1.878(4) Å in **2-Ag** and to 1.882(6) Å in **2-Au**. The M−C21 bond lengths (M = Ag, 2.122(3) Å; M = Au, 2.082(5) Å) are comparable to those in different coinage metal NHC complexes reported in the literature.[93,94] Note that compounds associating tantalum with silver or gold are exceedingly rare in the literature.[87] Only one complex, Ph$_3$PAuTa(CNDipp)$_6$ (Dipp = 2,6-diisopropylphen-

https://doi.org/10.1021/jacs.4c02172
J. Am. Chem. Soc. 2024, 146, 18306−18319

Table 1. Key Structural Parameters (Distances in Å and Angles in °) for 1, 2-Cu, 2-Ag, 2-Au, and 3-Au[a]

	1	2-Cu	2-Ag	2-Au	3-Au
Ta1−M	2.872(5)	2.7018(8)	2.95(3)	2.9462(3)	2.9376(4)
Ta1−C1	1.838(3)	1.844(2)	1.878(4)	1.882(6)	2.05(1)
Ta1−C6	2.170(3)	2.161(3)	2.17(1)	2.163(6)	1.921(8)
Ta1−C11	2.177(3)	2.167(2)	2.176(4)	2.172(6)	2.165(9)
Ta1−C16	2.220(3)	2.223(2)	2.202(3)	2.174(6)	2.184(8)
M−C1	/	2.011(2)	2.176(7)	2.032(5)	2.121(7)
M−C21	/	1.919(2)	2.122(3)	2.082(5)	2.046(7)
Ta1−M−C21	/	166.4(1)	161.3(4)	164.8(2)	144.6(2)
Ta1−C1−C2	166.4(2)	157.3(2)	157(2)	149.8(4)	135.8(6)
Ta1−C6−C7	131.2(2)	132.7(2)	136(2)	132.9(2)	166.1(7)

[a]For **2-Ag**, average values between both molecules found in the asymmetric unit. M = Li, Cu, Ag, or Au.

Scheme 2. Salt Metathesis Preparation of the Heterobimetallic Complexes $[Ta(CH_2tBu)_3(\mu\text{-}CtBu)_2M(IPr)]$, 2-M (M = Cu, Ag, Au, IPr = 1,3-Bis(2,6-diisopropylphenyl)imidazol-2-ylidene)

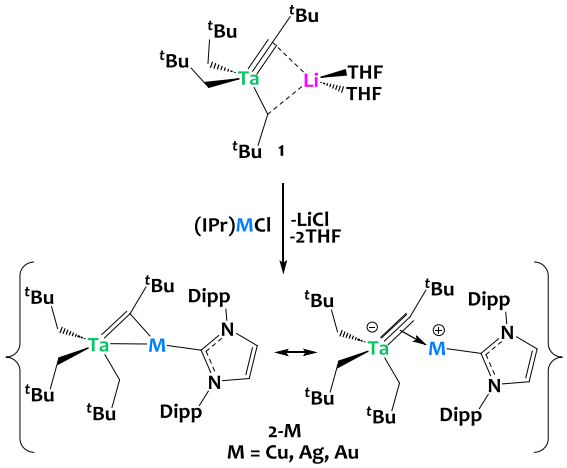

Two extreme resonance forms are shown.

yl), which features an unsupported metal−metal bond of 2.7207(2) Å,[95] is reported in the CCDC database.

Interestingly, we observed that, in C_6D_6 solution (or toluene-d_8), complexes **2-M** slowly tautomerize into **3-M** $[Ta(CHtBu)(CH_2tBu)_2(\mu\text{-}CHtBu)M(IPr)]$ (M = Cu, Ag, Au, Scheme 3-top). Such alkylidyne alkyl to bis(alkylidene) tautomerism equilibrium (Scheme 3-bottom) is a rare phenomenon. Such a rearrangement was first postulated by Schrock and coworkers to account for the quantitative formation of $TaCp(CHtBu)_2(PMe_3)$ from treating $TaCp(CtBu)Cl(PMe_3)_2$ with $Mg(CH_2tBu)_2(dioxane)$[102] and has then been documented in a few cases with W and Os derivatives.[96−101] In these examples from literature, the relative stability of each tautomer depends on the nature of ancillary ligands, yet structural preference is difficult to predict and control. Still, in the case of $(Me_3SiCH_2)_3W{=}CSiMe$, Xue and coworkers have demonstrated that the coordination of external phosphine ligands such as PMe_3 could trigger this tautomeric equilibrium, helping to stabilize of the bis(alkylidene) tautomer $(Me_3SiCH_2)_2W(=CHSiMe_3)_2(PMe_3)$.[98,99] It is important to mention here that C_6D_6 solutions of compound **1** are stable over time at room temperature, and that the bis(alkylidene) tautomer is not observed in the absence of coinage metals.

Significantly, our findings reveal that the tautomeric equilibrium is not only initiated but also remarkably influenced by the choice of the coinage metal, as illustrated in Figure 3. In the heterobimetallic Ta/Cu system, the equilibrium in C_6D_6 solution at 30 °C predominantly favors the formation of complex **2-Cu** (**2-Cu**:**3-Cu** ratio at equilibrium 71%:29%). In contrast, within the Ta/Ag system, the equilibrium shifts toward **3-Ag**, with an equilibrium ratio of 31 to 69% in favor of **3-Ag** over **2-Ag** at 30 °C. This shift is even more pronounced in the Ta/Au system, where the equilibrium ratio between **2-Au** and **3-Au** is 6% to 94%, demonstrating a significant preference for the formation of **3-Au** over **2-Au**. These findings underscore the sensitivity of the tautomeric equilibrium to the specific late metal component in the complex, offering a valuable avenue for controlling this phenomenon.

Complexes **3-Cu** and **3-Ag** were characterized in the reaction mixture by conducting a comparative analysis of ^{13}C NMR spectra at both the initial time (t = 0) and at equilibrium (at 298 K). The formation of the new copper carbene species, **3-Cu**, was evidenced by the appearance of an additional Cu−C_{NHC} signal at 183.16 ppm, in addition to that found for **2-Cu** at 185.57 ppm (Figure 4b). ^{13}C NMR studies suggest that the two alkylidene ligands in **3-Cu** are fluxional in solution, which is manifested by the appearance of a broad signal centered at 205.75 ppm (Figure 4c). This value falls in the lower end of the range typical for Ta(V) neopentylylidenes.[71,72,74] Similar observations were made for the **2-Ag**/**3-Ag** equilibrium mixture; yet, in this case, the ^{13}C NMR signals display fine structure due to coupling with naturally abounding spin 1/2 ^{107}Ag and ^{109}Ag isotopes. Consequently, the C_{NHC} signal in **3-Ag** appears as a doublet of doublets at 190.59 ppm ($^1J_{Ag-C}$ = 145.4 and 167.0 Hz for ^{107}Ag and ^{109}Ag, respectively, see Figure 4f), in agreement with the literature.[93,103] The neopentylidene signal in **3-Ag** is observed as a broad doublet, displaying a coupling constant of 30.3 Hz with silver (Figure 4f). These observations confirm the interaction of silver with the NHC and both neopentylidene moieties in **3-Ag** on the NMR time scale.

Due to the pronounced equilibrium preference for **3-Au**, we successfully isolated and characterized it independently. At room temperature, the NMR signals of complex **3-Au** displayed significant broadening, presenting challenges in their assignment. This phenomenon is attributed to the rapid exchange between the two Ta=CHtBu motifs at the NMR time scale (see the VT ^1H NMR data in Figure S37). Cooling the sample to 253 K resulted in the emergence of three distinct sharp signals in the carbene region at 229.51, 202.23, and 167.59 ppm, corresponding to the TaCHtBu, AuC_{NHC}, and

https://doi.org/10.1021/jacs.4c02172
J. Am. Chem. Soc. 2024, 146, 18306−18319

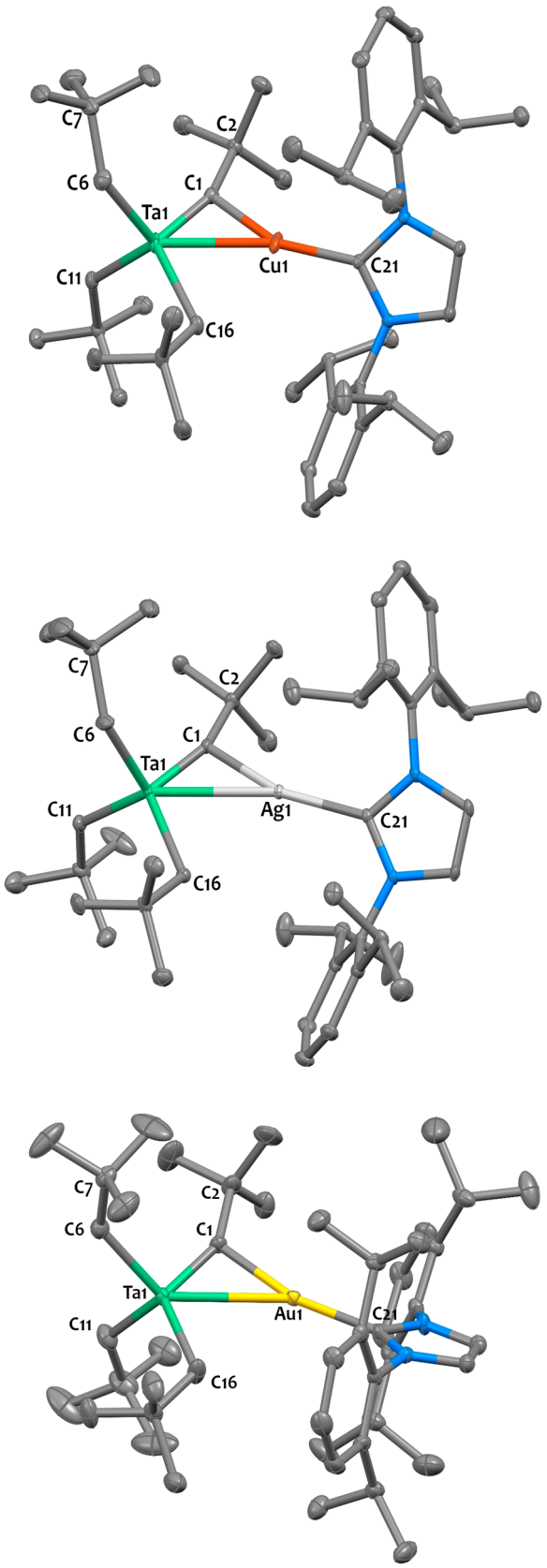

Figure 2. X-ray determined solid state structures for **2-Cu** (top), **2-Ag** (middle), and **2-Au** (bottom). Ellipsoids are represented with 30% probability. Disorder and hydrogen atoms have been omitted for clarity. Two independent molecules were found in the asymmetric unit of **2-Ag** (Z′ = 2), but one of them has been omitted for clarity. Selected distances (Å) and angles (deg) for **2-Cu**: Ta1−Cu1 2.7018(8), Ta1−C1 1.844(2), Ta1−C6 2.161(3), Ta1−C11 2.167(2), Ta1−C16 2.223(2), Cu1−C1 2.011(2), Cu1−C21 1.919(2), Ta1−Cu1−C21 166.4(1), Ta1−C1−C2 157.3(2), Ta1−C6−C7 132.7(2); for **2-Ag**: Ta1−Ag1 2.95(3), Ta1−C1 1.878(4), Ta1−C6 2.17(1), Ta1−C11 2.176(4), Ta1−C16 2.202(3), Ag1−C1 2.176(7), Ag1−C21 2.122(3), Ta1−Ag1−C21 161.3(4), Ta1−C1−C2 157(2), Ta1−C6−C7 136(2); for **2-Au**: Ta1−Au1 2.9462(3), Ta1−C1 1.882(6), Ta1−C6 2.163(6), Ta1−C11 2.172(6), Ta1−C16 2.174(6), Au1−C1 2.032(5), Au1−C21 2.082(5), Ta1−Au1−C21 162.8(2), Ta1−C1−C2 149.8(4), Ta1−C6−C7 132.9(2).

Scheme 3. (Top) Equilibrium between the Alkylidyne-Bridged Species 2-M and Alkylidene-Bridged Species, 3-M (M = Cu, Ag, Au); (Bottom) Alkyl Alkylidyne/Bis-alkylidene Tautomerism Equilibrium[96−101]

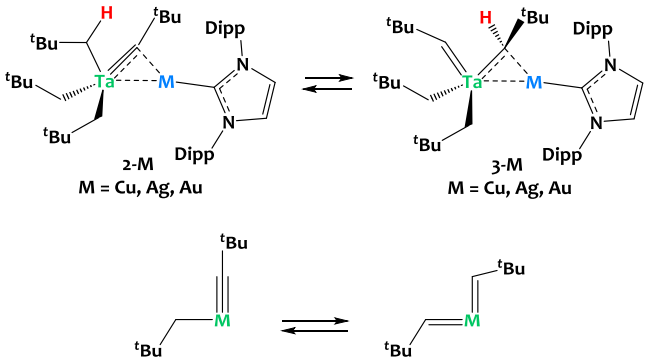

Ta(μ-CH*t*Bu)Au motifs, respectively (see Figure 4d), consistent with the proposed molecular structure. The bridging neopentylidene ^{13}C NMR resonance is strongly high-field shifted compared to the nonbridging neopentylidene moiety, as was reported previously in a TaRh(μ-CH*t*Bu) species (δ= +170.1 ppm).[71] Note that the neopentylidene α-H resonances observed in the ^{1}H NMR spectra of complexes **3-M** (M = Cu, Ag, Au) appear in very upfield regions (1.5−2.2 ppm). Although typical values are comprised between +3 and +7 ppm,[71,74,104,105] there are a number of examples that deviate from this range, demonstrating upfield resonances. For instance, in compound Ta(=CH*t*Bu)(CH_2*t*Bu)$_3$, the α-H signal of the neopentylidene ligand in C_6D_6 solution at room temperature appears at +1.9 ppm.[107,106] Similarly, in other compounds such as [Li][{Ta(CH*t*Bu)(CH_2*t*Bu)$_2$}-{IrH_2Cp^*}],[72] Tp′Ta(NMe_2)(CH*t*Bu)Cl, and Tp′Ta(CH*t*Bu)-Br_2,[108] the neopentylidene resonance is found at +0.98; +1.68, and +1.88 ppm, respectively.

Additionally, **3-Au** was crystallized from pentane through slow evaporation, and the solid-state structure was elucidated using single crystal X-ray diffraction (Figure 5). The Ta1−C1 distance in **3-Au** (2.05(1) Å) is significantly elongated compared to that in **2-Au** (1.882(6) Å), and the Ta1−C6 bond length is shortened (1.921(8) Å in **3-Au** vs 2.163(6) Å in **2-Au**), as expected. As a result of H transfer, the geometry around the C1 center shifts from pseudo trigonal planar in **2-Au**, to pseudo tetrahedral in **3-Au**, as shown by the mean deviation of C1 atom from the Ta1−Au1−C2 plane (0.01(1) Å in **2-Au** vs 0.49(1) Å in **3-Au**). The Ta1−C6−C7 angle is increased, from 132.9(2)° in **2-Au** to 166.1(7)° in **3-Au**. Such obtuse angle is frequently observed in primary alkylidenes,[71,74,84,109] as a result of C−H agostic interaction, further confirming the bis-alkylidene nature of complex **3-Au**. Note

https://doi.org/10.1021/jacs.4c02172
J. Am. Chem. Soc. 2024, 146, 18306−18319

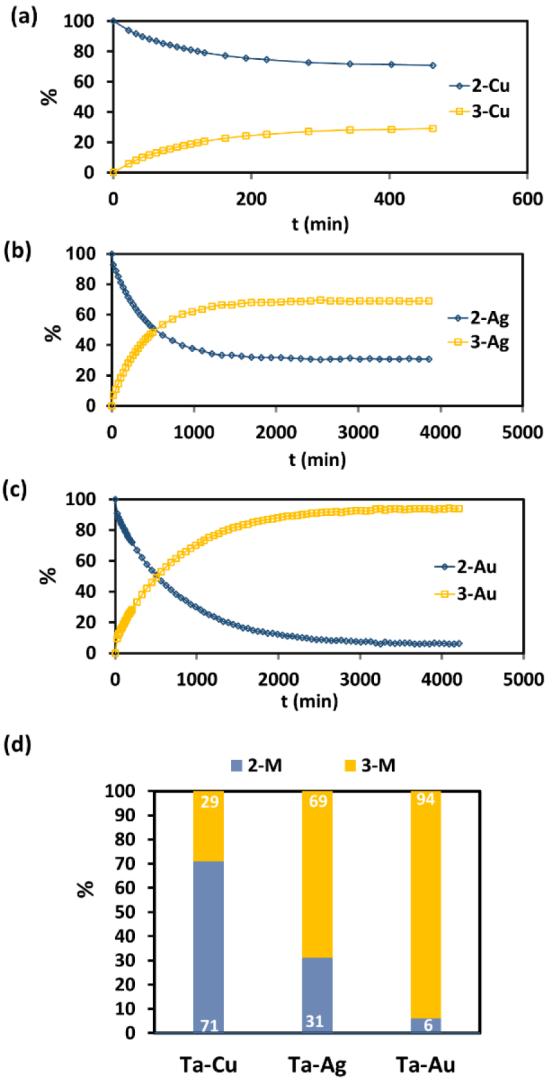

Figure 3. (a–c) Evolution in the percentages of complexes **2-M** and **3-M** as a function of time in C_6D_6 solution at 303 K. (d) **2M:3M** ratio at equilibrium. The equilibrium position is shifted as we move down the group 11 metal column, favoring the tantalum bis-neopentylidene over tantalum neopentyl neopentylidyne tautomer.

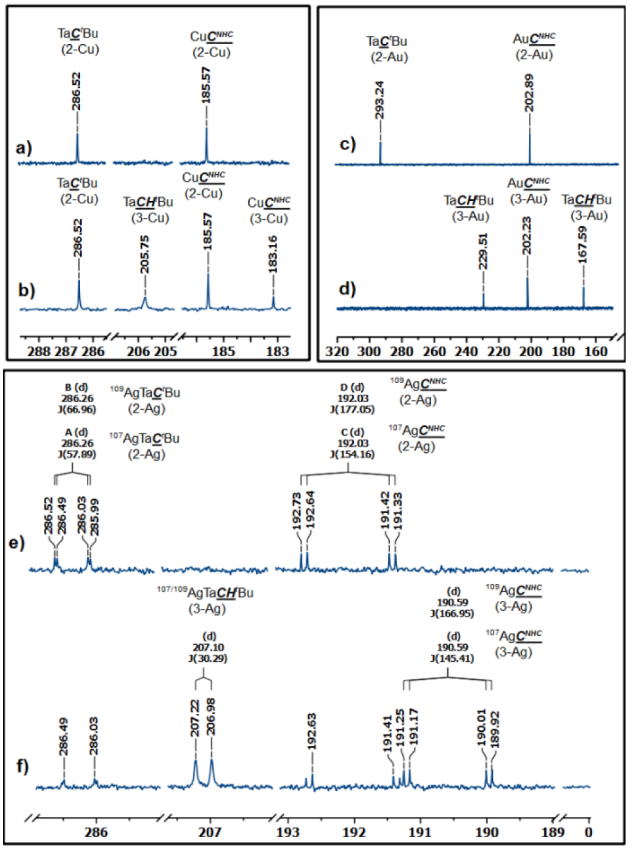

Figure 4. $^{13}C\{^1H\}$-NMR (126 MHz) spectra of (a) compound **2-Cu** in C_6D_6 at 298 K, (b) equilibrium mixture of **2-Cu** and **3-Cu** in C_6D_6 at 298 K, (c) compound **2-Au** in C_6D_6 at 298 K, (d) compound **3-Au** in toluene-d^8 at 253 K, (e) compound **2-Ag** in C_6D_6 at 298 K, (f) equilibrium mixture of **2-Ag** and **3-Ag** in C_6D_6 at 298 K.

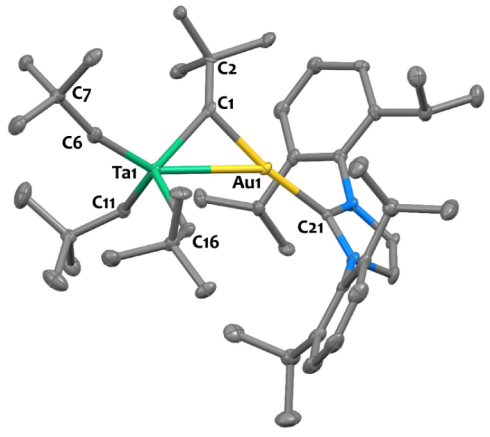

Figure 5. X-ray determined solid-state structure for complex **3-Au**. Ellipsoids are represented with 30% probability. Hydrogen atoms have been omitted for clarity. Selected distances (Å) and angles (deg): Ta1–Au1 2.9376(4), Ta1–C1 2.05(1), Ta1–C6 1.921(8), Ta1–C11 2.165(9), Ta1–C16 2.184(8), Au1–C1 2.121(7), Au1–C21 2.046(7), Ta1–Au1–C21 144.6(2), Ta1–C1–C2 135.8(6), Ta1–C6–C7 166.1(7).

that the presence of this agostic interaction is confirmed by DFT calculations, showing short Au–H distance and elongated C–H distance in the computed structure for **3-Au** (see Figure DFT-7 in Supporting Information). In NBO analysis, we also see a stronger donation of the C–H bond to the Ta center for **3-Au**. The distance between the Au atom and the Ta–C1 multiple bond centroid is almost identical in **2-Au** (2.37(1) Å) and **3-Au** (2.35 Å). This tends to suggest that the π-bonding of the gold center to the tantalum carbon multiple bonds is similar in both tautomers.

To better understand this phenomenon, DFT calculations were carried out (B3PW91 functional) including or not dispersion corrections. The optimized geometries of **2-Cu**, **2-Ag**, **2-Au**, and **3-Au** compare well with the experimental ones (see Supporting Information). The reaction profile for the tautomerism reaction (Figure 6) implies a Ta-assisted hydrogen transfer from the neopentyl to the alkylidyne. The computed barrier is in the 30–31 kcal·mol^{-1} range depending on the metal, in line with the lack of inclusion of the coinage metal at the transition state. It is interesting to note that the formation of **3-Cu** from **2-Cu** is slightly endothermic by 0.8 kcal·mol^{-1}, which fits with the experimental observation of **2-Cu** being more stable than **3-Cu** (experimental ratio **2-Cu:3-Cu** 71%:29%). In the Ag and Au cases, the formation of **3-Ag** and **3-Au** is exothermic by 0.1 and 1.4 kcal·mol^{-1}, respectively,

https://doi.org/10.1021/jacs.4c02172
J. Am. Chem. Soc. 2024, 146, 18306–18319

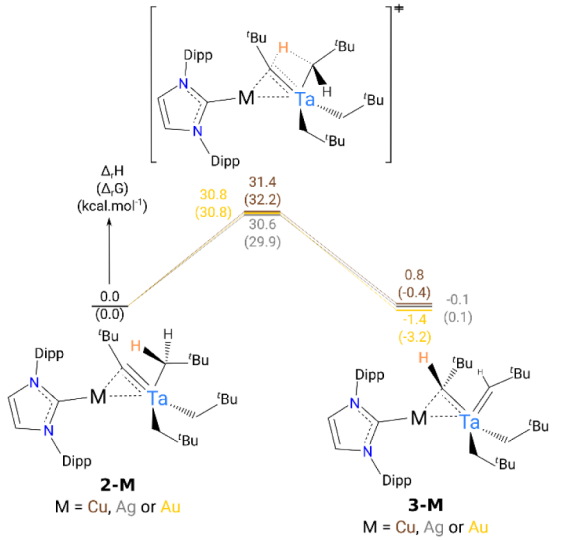

Figure 6. Computed energy profile at room temperature for the tautomerism reaction **2-M** ⇌ **3-M**. The energies are given in kcal·mol^{-1}.

in line with the experimental observation (**2-M**:**3-M** ratio for M = Ag 31%:69% and for M = Au 6%:94%). It is interesting to notice that the inclusion of the dispersion correction does not improve the result and even does not fit with the experimental thermodynamic parameters (the reaction is becoming very endothermic for Cu). Analyses of the computed metrical parameters and charges suggest that the Au−$C_{carbyne}$ interaction is weaker than the Ag−$C_{carbyne}$ and Cu−$C_{carbyne}$ interactions. This trend is corroborated by natural charge calculations (see Figure DFT-5 in Supporting Information), where, overall, the charge on gold (+0.31) is smaller than those on Ag (+0.44) and Cu (+0.46) in compounds **2-M**, which could promote such tautomerism.

To illustrate the potential of these new bimetallic architectures to promote cooperative reactivity, we studied the reaction of complexes **2-M** with a CO_2 atmosphere (ca. 0.7 mbar, 2 equiv). The reaction was carried out in pentane at −80 °C for 10 min and then at room temperature for 1h. This led to the precipitation of the ketenyl complexes, (^{t}BuCCO)M(IPr), **4-M** (M = Cu, Ag, Au, see Scheme 4), which were

Scheme 4. Reaction of Compounds 2-M with CO_2 Producing the Ketenyl Complexes (^{t}BuCCO)M(IPr), 4-M (M = Cu, Ag, Au)

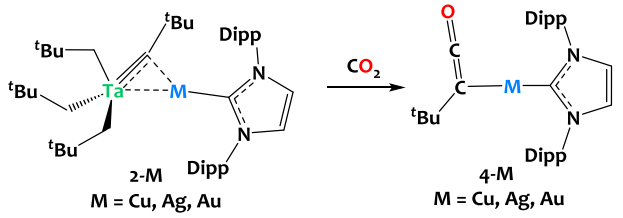

isolated as white solids in 48% to 77% yields. The moderate yield is attributed, at least in part, to the partial solubility of compounds **4-M** in pentane, which is employed for washing the materials.

Complexes **4-M** were fully characterized by NMR and IR spectroscopy. The ^{1}H NMR spectra show a singlet at δ = 1.15 ppm attributed to the *t*Bu group in **4-Cu** (corresponding signal found at δ = 1.21 and 1.16 ppm for **4-Ag** and **4-Au**, respectively). In the ^{13}C NMR spectra, the ketenyl moiety gives rise to characteristic signals at δ = 169.89, 169.38, and 181.19 ppm for the central C atom and δ = 24.39, 23.70, and 32.00 ppm for C_α in **4-Cu**, **4-Ag**, and **4-Au**, respectively.[61,110−112] The C_{NHC} ^{13}C NMR signals are found at 183.83 ppm for **4-Cu**, 189.20 ppm for **4-Ag**, and 193.39 ppm for **4-Au**, as expected.[80] In the DRIFT spectra, the strong absorption bands at 2012 cm^{-1} for **4-Cu**, 2016 cm^{-1} for **4-Ag**, and 2027 cm^{-1} for **4-Au** confirm the presence of the ketenyl fragment (see Figure S66). This infrared ν(CCO) absorption is red-shifted in comparison to the typical range for ketenes (2120−2070 cm^{-1}).[62,113−115] For comparison, in the related compounds [M](CCO)*t*Bu (where [M] = Et_3Ge, Bu_3Sn), the corresponding stretches appear at 2070 and 2060 cm^{-1}, respectively,[110] and two recent articles describing ketenyl derivatives reported ν(CCO) absorptions at 2047 and 2030 cm^{-1}.[61,64]

Conclusive evidence of the ketenyl moiety arises from the X-ray diffraction structure of compound **4-Cu**, which is shown in Figure 7. The short C1−C2 and C2−O1 bond lengths as well

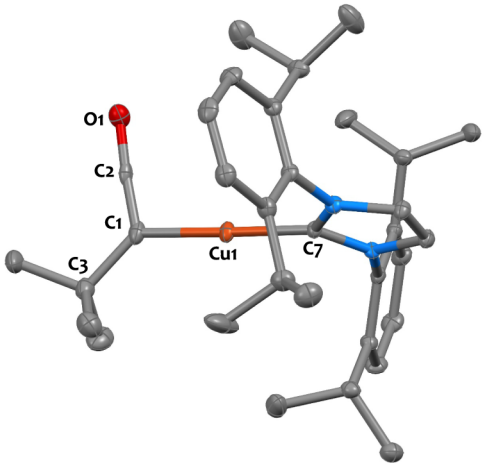

Figure 7. X-ray determined solid state structure for compound **4-Cu**. Ellipsoids are represented with 30% probability. Hydrogen atoms have been omitted for clarity. Selected distances (Å) and angles (deg): Cu1−C1 1.908(4), Cu1−C7 1.891(4), C1−C2 1.273(7), C2−O1 1.201(6), C1−C3 1.542(7), C1−Cu1−C7 176.5(2), C1−C2−O1 174.8(4), C3−C1−C2 126.0(4).

as wide C1−C2−O1 angle (1.273(7) Å, 1.201(6) Å, and 174.8(4)°, respectively) support assignment as a η^1C(*t*Bu)═C═O ketenyl motif.[61,62,66,113,116] The Cu(I) center adopts a linear geometry (C1−Cu1−C7 angle = 176.5(2)°), and the Cu1−C1 and Cu1−C7 bond lengths (1.908(4) Å and 1.891(4) Å, respectively) are akin that found in NHC copper(I) aryl complexes.[117]

Ketenyl compounds have been relatively scarce in the scientific literature, even though there has been a notable surge in interest in the past years.[60−66] Copper and silver ketenyl species have been proposed and debated as pivotal intermediates within catalytic cycles, for instance in the Kinugasa reaction.[33,67−70] Despite their theoretical significance, these species remained elusive and were never isolated to the best of our knowledge, underscoring the scientific interest and relevance of compounds **4-M**.

The originality of this family of ketenyl compounds is not confined to its structural features; it also extends to the

https://doi.org/10.1021/jacs.4c02172
J. Am. Chem. Soc. 2024, 146, 18306−18319

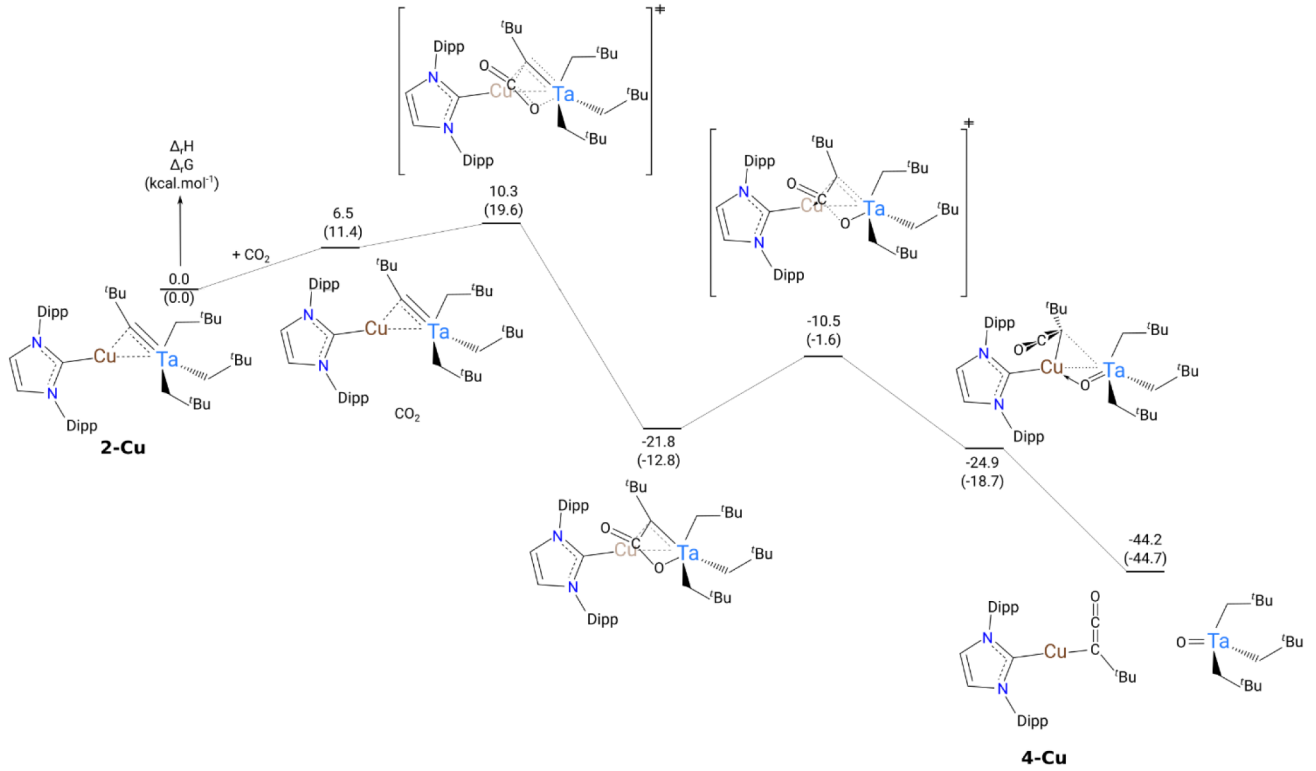

Figure 8. Computed reaction pathway of the formation of **4-Cu** at room temperature. The energies are given in kcal·mol^{-1}.

uniqueness of its synthetic route. Traditionally, the prevalent approach to synthesizing ketenyl species relies on their preparation from carbon monoxide (CO). To the best of our knowledge, only one example of carbon dioxide cleavage leading to the formation of a ketenyl fragment was described in the literature.[118] The proposed mechanism involves initial CO_2 cycloaddition on a tungsten alkylidyne complex, $[CF_3{-}ONO]W{=}CC(t)Bu(THF)_2$, to generate a heterometallacyclobutene, which then rearranges to yield a tungsten-oxo and the ketenyl moiety in $[CF_3{-}ONO]W{=}O[C(t)BuCO]$. A comparable mechanism may be proposed here, involving the putative formation of a $[(CH_2t\text{Bu})_3Ta{=}O]_n$ species and then subsequent transfer of the ketenyl moiety to the M(IPr) fragment (M = Cu, Ag, Au). Regrettably, our attempts to definitely identify or isolate this tantalum-oxo coproduct were unsuccessful despite major efforts, primarily due to the very high solubility of the compound and the likelihood of it adopting various oligomeric structures in solution. In light of the burgeoning of emerging and novel heterobimetallic CO_2 cleavage pathways documented in the literature,[119−127] it is also conceivable that a concerted carbon dioxide activation may occur across the tantalum-coinage metal centers.

We further investigated the reaction of the Ta/Li carbyne complex **1** with CO_2 (2 equiv) in pentane under the same experimental conditions. This reaction yielded a precipitate, indicative of a chemical transformation taking place. However, the complexity of this reaction was evidenced by the analysis of this solid using ^{1}H NMR spectroscopy, which revealed the formation of a mixture comprising numerous species (see Figure S64). Despite our efforts, the identification of these products remained elusive. This observation underscores the complexity of the reaction mechanism and highlights the pivotal role played by the coinage metal partner in stabilizing the ketenyl fragment in this reaction.

To shed light on the possible mechanisms explaining the unusual formation of complex **4**, DFT calculations (B3PW91) have been performed (Figure 8). The reaction begins by the formation of a van der Waals adduct of CO_2 to **2-Cu**, which is endothermic by 6.5 kcal·mol^{-1}. To form this adduct, CO_2 has to open some space in between the Dipp and *t*Bu ligands explaining the positive enthalpy of formation. From this adduct, CO_2 undergoes a [2 + 2] cycloaddition on the Ta—C−*t*Bu bond with an associated low barrier (10.3 kcal·mol^{-1}). Following the intrinsic reaction coordinate, it yields to a stable metallacyclobutane-type intermediate (−21.8 kcal·mol^{-1}). In this intermediate, the carbon of the former alkylidene interacts with both Ta and Cu, while the carbon of CO_2 is not interacting with any metal. The coordination of the carbon of CO_2 to Cu allows the activation of the C−O bond of this stable intermediate. The associated barrier is 11.3 kcal·mol^{-1} in line with a kinetically facile reaction. This ultimately yields complex **4-Cu** and the formation of a Ta═O complex, which are found to be highly stable (−44.2 kcal·mol^{-1}).

CONCLUSION

A salt metathesis synthetic strategy has been used with success to access rare tantalum/coinage metals heterobimetallic complexes $[Ta(CH_2t\text{Bu})_3(\mu\text{-}Ct\text{Bu})M(IPr)]$ **2-M** (M = Cu, Ag, Au, IPr = 1,3-bis(2,6-diisopropylphenyl)imidazol-2-ylidene) in high yields. Despite the large body of fundamental work dedicated to the study of transition metal alkylidene and alkylidyne complexes, the alkylidyne/alkyne tautomerism equilibrium is a rarely observed phenomenon. Here, we show for the first time that the addition of an external coinage metal center, with affinity for π-bonding to the tantalum−carbon multiple bond, can be used as a strategy to trigger and tune this unusual tautomerism equilibrium (Cu < Ag < Au).

https://doi.org/10.1021/jacs.4c02172
J. Am. Chem. Soc. 2024, 146, 18306−18319

Given the importance of metal alkyllidynes/alkylidenes in catalysis, this work could open new avenues for reactivity.

Furthermore, we show that these uncommon heterobimetallic complexes could open attractive opportunities for synergistic reactivity. We notably report an unusual deoxygenative carbyne transfer to CO_2 resulting in rare examples of coinage metal ketenyl species, (^{t}BuCCO)M(IPr), **4-M** (M = Cu, Ag, Au). Interestingly, in the case of the Ta/Li analogue **1**, the bis(alkylidene) tautomer is not detected, and the reaction with CO_2 does not cleanly yield ketenyl species, which highlights the pivotal role played by the coinage metal partner in controlling these unconventional reactions. This innovative reactivity could open up new avenues for exploring various synthetic possibilities in the fast-growing field of ketenyl species.

EXPERIMENTAL SECTION

General Considerations. Unless otherwise noted, all reactions were performed either using standard Schlenk line techniques or in an MBRAUN glovebox under an atmosphere of purified argon (<1 ppm of O_2/H_2O). Glassware and cannulas were stored in an oven at ∼100 °C for at least 16 h prior to use. THF and *n*-pentane were purified by passage through a column of activated alumina, dried over Na/benzophenone, vacuum-transferred to a storage flask, and freeze−pump−thaw degassed prior to use. Deuterated solvents (toluene-d_8, THF-d_8, and C_6D_6) were dried over Na/benzophenone, vacuum-transferred to a storage flask, and freeze−pump−thaw degassed prior to use. Compound [Ta($CH_2{}^t$Bu)$_3$(CH^tBu)] was prepared according to the literature procedure.[52] All other reagents were acquired from commercial sources and used as received.

IR Spectroscopy. The samples were prepared in a glovebox (diluted in dry KBr), sealed under argon in a DRIFT cell fitted with KBr windows, and then analyzed using a Nicolet 670 FT-IR spectrometer.

Elemental Analyses. Elemental analyses were performed under an inert atmosphere at Mikroanalytisches Labor Pascher, Germany.

X-Ray Structural Determinations. Experimental details regarding single-crystal XRD measurements are provided in the Supporting Information. CCDC 2310994−2310999 contain supplementary crystallographic data for this article. These data can be obtained free of charge from The Cambridge Crystallographic Data Centre viawww.ccdc.cam.ac.uk/structures.

NMR Spectroscopy. Solution NMR spectra were recorded on Bruker AV-300 and AV-500 spectrometers. ^{1}H and ^{13}C chemical shifts were measured relative to residual solvent peaks, which were assigned relative to an external TMS standard set at 0.00 ppm. ^{1}H and ^{13}C NMR assignments were confirmed by ^{1}H−^{1}H COSY, ^{1}H−^{13}C HSQC, and HMBC experiments. NMR data recorded as follows: chemical shift (δ) [multiplicity, coupling constant(s) J (Hz), relative integral], where multiplicity is defined: s = singlet, d = doublet, t = triplet, q = quartet, m = multiplet or combinations thereof, and prefixed br = broad.

Synthesis of [Li(THF)$_2$][Ta($CH_2{}^t$Bu)$_3$(C^tBu)] (1). This synthesis was adapted from a published procedure.[52] A 0.77 mL hexane solution of *n*-BuLi (1.6 M, 1.23 mmol, 1.1 equiv) was added dropwise, at −40 °C, to a 10 mL orange pentane solution of [Ta($CH_2{}^t$Bu)$_3$(CH^tBu)] (500 mg, 1.08 mmol, 1.0 equiv) and THF (0.35 mL, 4.32 mmol, 4.0 equiv). The resulting solution was stirred at room temperature for 1 h. Then, the volatiles were removed under vacuum, yielding a yellow solid. This powder was dissolved in the minimum amount of pentane (ca. 6 mL) and stored at −40 °C for 16 h, yielding after filtration and drying under vacuum compound **1** as orange crystals (412 mg, 62% yield). ^{1}H NMR (300 MHz, C_6D_6, 298 K) δ ppm 3.56 (m, 8H, THF), 1.61 (s, 9H, CC($C\underline{H}_3$)$_3$), 1.44 (s, 27H, 3 $CH_2C(C\underline{H}_3)_3$), 1.35 (m, 8H, THF), 0.65 (s, 6H, 3 $C\underline{H}_2$Ta). ^{13}C{^{1}H}-NMR (126 MHz, C_6D_6, 298 K) δ ppm 281.77 (br s, 1C, Ta$\underline{C}$C(CH_3)$_3$), 101.46 (s, 3C, Ta$\underline{C}H_2C(CH_3)_3$), 68.88 (s, 4C, THF), 50.74 (s, 1C, TaC$\underline{C}$(CH_3)$_3$), 36.99 (s, 3C, TaCC($\underline{C}H_3$)$_3$), 36.22 (s, 9C, $TaCH_2C(\underline{C}H_3)_3$), 35.00 (s, 3C, $TaCH_2\underline{C}(CH_3)_3$), 25.37 (s, 4C, THF). Anal. calcd for $C_{28}H_{58}LiO_2Ta$: C, 54.71; H, 9.51. Found: C, 54.84; H, 9.52.

Synthesis of [Ta($CH_2{}^t$Bu)$_3$(μ-C^tBu)Cu(IPr)] (2-Cu). A 10 mL pentane solution of [Li(THF)$_2$][Ta($CH_2{}^t$Bu)$_3$(C^tBu)] (300 mg, 0.49 mmol, 1.0 equiv) was added dropwise at room temperature to a suspension of (IPr)CuCl (237 mg, 0.49 mmol, 1.0 equiv) in 4 mL of pentane. The resulting solution was stirred at room temperature for 1 h. The solution was filtered to remove the white LiCl precipitate. Then, the volatiles were removed under vacuum, yielding **2-Cu** as an orange solid (415 mg, 93% yield). Orange block single crystals of **2-Cu** suitable for XRD studies were grown by slow recrystallization of a pentane saturated solution at −40 °C over a period of 16 h. ^{1}H NMR (500 MHz, C_6D_6, 298 K) δ ppm 7.21−7.14 (m, 2H, 2 *para* C$\underline{H}^{Ar}$), 7.09 (d, $^3J_{1H-1H}$ = 7.7 Hz, 4H, 4 *meta* C$\underline{H}^{Ar}$), 6.46 (s, 2H, N−C$\underline{H}$═C$\underline{H}$-N), 3.04 (*hept*, $^3J_{1H-1H}$ = 6.8 Hz, 4H, 4 C$\underline{H}$(CH_3)$_2$), 1.40 (d, $^3J_{1H-1H}$ = 6.8 Hz, 12H, 2 CH($C\underline{H}_3$)$_2$), 1.38 (s, 9H, TaCC($C\underline{H}_3$)$_3$), 1.28 (s, 27H, $TaCH_2C(C\underline{H}_3)_3$), 1.00 (d, $^3J_{1H-1H}$ = 6.8 Hz, 12H, 2 CH($C\underline{H}_3$)$_2$), 0.68 (s, 6H, 3 $TaC\underline{H}_2C(CH_3)_3$). ^{13}C{^{1}H}-NMR (126 MHz, C_6D_6, 298 K) δ ppm 286.52 (s, 1C, Ta$\underline{C}$C(CH_3)$_3$), 185.57 (s, 1C, Cu$\underline{C}^{NHC}$), 145.17 (s, 4C, 4 $\underline{C}^{Ar}$*i*Pr), 136.38 (s, 2C, 2 $\underline{C}^{Ar}$N), 130.32 (s, 2C, 2 *para*$\underline{C}H^{Ar}$), 124.89 (s, 4C, 4 *meta*$\underline{C}H^{Ar}$), 123.13 (s, 2C, *N*−$\underline{C}$H═$\underline{C}$H−N), 104.79 (s, 3C, 3 $TaCH_2C(CH_3)_3$), 51.03 (s, 1C, TaC$\underline{C}$(CH_3)$_3$), 37.76 (s, 3C, TaCC($\underline{C}H_3$)$_3$), 36.08 (s, 9C, 3 $TaCH_2C(\underline{C}H_3)_3$), 35.33 (s, 3C, 3 $TaCH_2\underline{C}(CH_3)_3$), 28.92 (s, 4C, 4 $\underline{C}H^{iPr}$), 25.27 (s, 4C, 4 $\underline{C}H_3{}^{iPr}$), 23.98 (s, 4C, 4 $\underline{C}H_3{}^{iPr}$). Anal. calcd for $C_{47}H_{78}CuN_2Ta$: C, 61.65; H, 8.59; N, 3.06. Found: C, 61.54; H, 8.47; N, 3.03.

Synthesis of [Ta($CH_2{}^t$Bu)$_3$(μ-C^tBu)Ag(IPr)] (2-Ag). A 6 mL pentane solution of [Li(THF)$_2$][Ta($CH_2{}^t$Bu)$_3$(C^tBu)] (200 mg, 0.32 mmol, 1.0 equiv) was added dropwise to a suspension of (IPr)AgCl (168.6 mg, 0.32 mmol, 1.0 equiv) in 4 mL of pentane. The resulting solution was stirred at room temperature for 1 h. The solution was filtered to remove the white precipitate (LiCl). Then, the volatiles were removed under vacuum, yielding **2-Ag** as an orange solid (280 mg, 92% yield). Orange block single crystals of **2-Ag** suitable for XRD studies were grown by slow recrystallization of a pentane saturated solution at −40 °C over a period of 16 h. ^{1}H NMR (500 MHz, C_6D_6, 298 K) δ ppm 7.25−7.18 (m, 2H, 2 *para* C$\underline{H}^{Ar}$), 7.09 (d, $^3J_{1H-1H}$ = 7.8 Hz, 4H, 4 *meta* C$\underline{H}^{Ar}$), 6.39 (d, $^4J_{13C-109Ag}$ = $^4J_{13C-107Ag}$ = 1.0 Hz, 2H, N−C$\underline{H}$═C$\underline{H}$−N), 2.78 (hept, $^3J_{1H-1H}$ = 6.8 Hz, 4H, C$\underline{H}$(CH_3)$_2$), 1.43−1.31 (m, 21H, 2 CH($C\underline{H}_3$)$_2$ and TaCC($C\underline{H}_3$)$_3$), 1.29 (s, 27H, $TaCH_2C(C\underline{H}_3)_3$), 1.02 (d, $^3J_{1H-1H}$ = 6.9 Hz, 12H, 2 CH($C\underline{H}_3$)$_2$), 0.74 (s, 6H, 3 $TaC\underline{H}_2C(CH_3)_3$). ^{13}C{^{1}H}-NMR (126 MHz, C_6D_6, 298 K) δ ppm 286.26 (d, $^1J_{13C-109Ag}$ = 66.96 Hz and d, $^1J_{13C-107Ag}$ = 57.89 Hz, 1C, Ta$\underline{C}$C(CH_3)$_3$), 192.03 (d, $^1J_{13C-109Ag}$ = 177.05 Hz and d, $^1J_{13C-107Ag}$ = 154.16 Hz, 1C, Ag$\underline{C}^{NHC}$), 145.45 (s, 4C, 4 $\underline{C}^{Ar}$*i*Pr), 136.29 (br s, 2C, 2 $\underline{C}^{Ar}$N), 130.67 (s, 2C, 2 *para*$\underline{C}H^{Ar}$), 124.80 (s, 4C, 4 *meta*$\underline{C}H^{Ar}$), 123.43 (d, $^3J_{13C-109Ag}$ = $^3J_{13C-107Ag}$ = 4.85 Hz, 2C, *N*−$\underline{C}$H═$\underline{C}$H−N), 103.73 (d, $^2J_{13C-109Ag}$ = $^2J_{13C-107Ag}$ = 2.45 Hz, 3C, 3 $TaC\underline{C}H_2C(CH_3)_3$), 50.43 (d, $^2J_{13C-109Ag}$ = $^2J_{13C-107Ag}$ = 3.70 Hz, 1C, TaC$\underline{C}$(CH_3)$_3$), 38.44 (d, $^2J_{13C-109Ag}$ = $^2J_{13C-107Ag}$ = 3.40 Hz, 3C, TaCC($\underline{C}H_3$)$_3$), 36.15 (s, 9C, 3 $TaCH_2C(\underline{C}H_3)_3$), 35.30 (s, 3C, 3 $TaCH_2\underline{C}(CH_3)_3$), 28.89 (s, 4C, 4 $\underline{C}H^{iPr}$), 24.57 (s, 4C, 4 $\underline{C}H_3{}^{iPr}$), 24.39 (s, 4C, 4 $\underline{C}H_3{}^{iPr}$). Anal. calcd for $C_{47}H_{78}AgN_2Ta$: C, 58.81; H, 8.19; N, 2.92. Found: C, 58,97; H, 8,20; N, 2,95.

Synthesis of [Ta($CH_2{}^t$Bu)$_3$(μ-C^tBu)Au(IPr)] (2-Au). A 6 mL pentane solution [Li(THF)$_2$][Ta($CH_2{}^t$Bu)$_3$(C^tBu)] (200 mg, 0.32 mmol, 1.0 equiv) was added dropwise to a suspension of (IPr)AuCl (217 mg, 0.35 mmol, 1.1 equiv) in 4 mL of pentane. The resulting mixture was stirred at room temperature for 1 h. The solution was then filtered to remove the white precipitate (LiCl). Subsequently, the volatiles were removed under vacuum, yielding **2-Au** as an orange/brown solid (390 mg, 89% yield). Single crystals of **2-Au**, suitable for X-ray diffraction (XRD) studies, were grown by slow recrystallization of a pentane saturated solution at −40 °C over a period of 16 h. ^{1}H NMR (500 MHz, C_6D_6, 298 K) δ ppm 7.24 (t, $^3J_{1H-1H}$ = 7.8 Hz, 2H, 2 *para* C$\underline{H}^{Ar}$), 7.10 (d, $^3J_{1H-1H}$ = 7.8 Hz, 4H, 4 *meta* C$\underline{H}^{Ar}$), 6.33 (s, 2H, N−C$\underline{H}$═C$\underline{H}$-N), 2.85 (hept, $^3J_{1H-1H}$ = 6.9 Hz, 4H, C$\underline{H}$(CH_3)$_2$), 1.42 (d, $^3J_{1H-1H}$ = 6.9 Hz, 12H, 2 CH($C\underline{H}_3$)$_2$), 1.37 (s, 9H, TaCC($C\underline{H}_3$)$_3$), 1.28 (s, 27H, $TaCH_2C(C\underline{H}_3)_3$), 1.04 (d, $^3J_{1H-1H}$ = 6.8

https://doi.org/10.1021/jacs.4c02172
J. Am. Chem. Soc. 2024, 146, 18306−18319

Hz, 12H, 2 CH($C\underline{H}_3$)$_2$), 0.75 (s, 6H, 3 TaC$\underline{H}_2$C(CH_3)$_3$). $^{13}C\{^1H\}$-NMR (126 MHz, C_6D_6, 298 K) δ ppm 293.24 (s, 1C, Ta$\underline{C}$C(CH_3)$_3$), 202.89 (s, 1C, Au$\underline{C}^{NHC}$), 145.50 (s, 4C, 4 $\underline{C}^{Ar}$*i*Pr), 136.27 (s, 2C, 2 $\underline{C}^{Ar}$N), 130.66 (s, 2C, 2 *para*-$\underline{C}H^{Ar}$), 124.84 (s, 4C, 4 *meta*-$\underline{C}H^{Ar}$), 123.13 (s, 2C, *N*−$\underline{C}$H═$\underline{C}$H−N), 108.48 (s, 3C, 3 Ta$\underline{C}H_2$C(CH_3)$_3$), 50.21 (s, 1C, TaC$\underline{C}$(CH_3)$_3$), 38.45 (s, 3C, TaCC($\underline{C}H_3$)$_3$), 36.09 (s, 9C, 3 TaCH$_2$C($\underline{C}H_3$)$_3$), 35.89 (s, 3C, 3 TaCH$_2\underline{C}$(CH_3)$_3$), 28.93 (s, 4C, 4 $\underline{C}H^{iPr}$), 24.49 (s, 4C, 4 $\underline{C}H_3{}^{iPr}$), 24.15 (s, 4C, 4 $\underline{C}H_3{}^{iPr}$). Anal. calcd for $C_{47}H_{78}AuN_2Ta$: C, 53.81; H, 7.49; N, 2.67. Found: C, 54.02; H, 7.48; N, 2.63.

Characterization of [Ta($CH_2{}^tBu$)$_2$(μ-$CH{}^tBu$)$_2$Cu(IPr)] (3-Cu). This product could not be isolated, but was characterized from the equilibrium mixture of **2-Cu** and **3-Cu**. This mixture was obtained by dissolving 50 mg of complex **2-Cu** in 1 mL of C_6D_6 in a Young-type NMR tube and allowing it to sit at room temperature for 24 h. ^1H NMR (500 MHz, C_6D_6, 298 K) δ ppm 7.22−7.14 (m, 2H, 2 *para* C$\underline{H}^{Ar}$), 7.09 (d, $^3J_{1H-1H}$ = 8.1 Hz, 4H, 4 *meta* C$\underline{H}^{Ar}$), 6.33 (s, 2H, N−C$\underline{H}$═C$\underline{H}$−N), 2.81 (*hept*, $^3J_{1H-1H}$ = 6.8 Hz, 4H, 4 C$\underline{H}$(CH_3)$_2$), 1.48 (s, 2H, 2 TaC$\underline{H}$C(CH_3)$_3$), 1.42−1.35 (m, 30H, 2 CH($C\underline{H}_3$)$_2$ and 2 TaCHC($C\underline{H}_3$)$_3$), 1.34 (s, 18H, 2 TaCH$_2$C($C\underline{H}_3$)$_3$), 1.00 (d, $^3J_{1H-1H}$ = 6.8 Hz, 12H, 2 CH($C\underline{H}_3$)$_2$), 0.38 (s, 4H, 2 TaC$\underline{H}_2$C(CH_3)$_3$). $^{13}C\{^1H\}$-NMR (126 MHz, C_6D_6, 298 K) δ ppm 205.75 (s, 2C, 2 Ta$\underline{C}$HC(CH_3)$_3$), 183.16 (s, 1C, Cu$\underline{C}^{NHC}$), 145.40 (s, 4C, 4 $\underline{C}^{Ar}$*i*Pr), 135.62 (s, 2C, 2 $\underline{C}^{Ar}$N), 131.03 (s, 2C, 2 *para*C$\underline{H}^{Ar}$), 124.66 (s, 4C, 4 *meta*C$\underline{H}^{Ar}$), 123.33 (s, 2C, *N*−$\underline{C}$H═$\underline{C}$H−N), 93.43 (s, 2C, 2 Ta$\underline{C}H_2$C(CH_3)$_3$), 45.58 (s, 2C, 2 TaCH$\underline{C}$(CH_3)$_3$), 37.15 (s, 6C, 2TaCHC($\underline{C}H_3$)$_3$), 36.35 (s, 6C, 3 TaCH$_2$C($\underline{C}H_3$)$_3$), 34.17 (s, 2C, 2 TaCH$_2\underline{C}$(CH_3)$_3$), 28.92 (s, 4C, 4 $\underline{C}H^{iPr}$), 24.98 (s, 4C, 4 $\underline{C}H_3{}^{iPr}$), 24.10 (s, 4C, 4 $\underline{C}H_3{}^{iPr}$).

Characterization of [Ta($CH_2{}^tBu$)$_2$(μ-$CH{}^tBu$)$_2$Ag(IPr)] (3-Ag). This product could not be isolated but was characterized from the equilibrium mixture of **2-Ag** and **3-Ag**. This mixture was obtained by dissolving 50 mg of complex **2-Ag** in 1 mL of C_6D_6 in a Young-type NMR tube and allowing it to sit at room temperature for 24 h. ^1H NMR (500 MHz, C_6D_6, 298 K) δ ppm 7.26−7.20 (m, 2H, 2 *para* C$\underline{H}^{Ar}$), 7.07 (d, $^3J_{1H-1H}$ = 7.8 Hz, 4H, 4 *meta* C$\underline{H}^{Ar}$), 6.34 (d, $^4J_{13C-109Ag}$ = $^4J_{13C-107Ag}$ = 1.0 Hz 2H, N−C$\underline{H}$═C$\underline{H}$−N), 2.65 (*hept*, $^3J_{1H-1H}$ = 6.8 Hz, 4H, 4 C$\underline{H}$(CH_3)$_2$), 2.10 (s, 2H, 2 TaC$\underline{H}$C(CH_3)$_3$), 1.42−1.35 (m, 30H, 2 CH($C\underline{H}_3$)$_2$ and 2 TaCHC($C\underline{H}_3$)$_3$), 1.33 (s, 18H, 2 TaCH$_2$C($C\underline{H}_3$)$_3$), 1.02 (d, $^3J_{1H-1H}$ = 6.9 Hz, 12H, 2 CH($C\underline{H}_3$)$_2$), 0.47 (s, 4H, 2 TaC$\underline{H}_2$C(CH_3)$_3$). $^{13}C\{^1H\}$-NMR (126 MHz, C_6D_6, 298 K) δ ppm 207.10 (d, $^1J_{13C-109Ag}$ = $^1J_{13C-107Ag}$ = 30.29 Hz, 2C, Ta$\underline{C}H$C(CH_3)$_3$), 190.59 (d, $^1J_{13C-109Ag}$ = 166.95 Hz and d, $^1J_{13C-107Ag}$ = 145.41 Hz, 1C, Ag$\underline{C}^{NHC}$), 145.49 (s, 4C, 4 $\underline{C}^{Ar}$*i*Pr), 135.61 (br s, 2C, 2 $\underline{C}^{Ar}$N), 130.99 (s, 2C, 2 *para*$\underline{C}H^{Ar}$), 124.63 (s, 4C, 4 *meta*$\underline{C}H^{Ar}$), 123.37 (d, $^3J_{13C-109Ag}$ = $^3J_{13C-107Ag}$ = 4.74 Hz, 2C, *N*−$\underline{C}$H═$\underline{C}$H−N), 94.63 (s, 2C, 2 Ta$\underline{C}H_2$C(CH_3)$_3$), 45.00 (d, $^2J_{13C-109Ag}$ = $^2J_{13C-107Ag}$ = 1.10 Hz, 2C, TaCH$\underline{C}$(CH_3)$_3$), 37.20 (d, $^2J_{13C-109Ag}$ = $^2J_{13C-107Ag}$ = 1.20 Hz, 6C, TaCHC($\underline{C}H_3$)$_3$), 35.62 (s, 6C, 2 TaCH$_2$C($\underline{C}H_3$)$_3$), 34.07 (s, 2C, 2 TaCH$_2\underline{C}$(CH_3)$_3$), 28.97 (s, 4C, 4 $\underline{C}H^{iPr}$), 24.70 (s, 4C, 4 $\underline{C}H_3{}^{iPr}$), 24.40 (s, 4C, 4 $\underline{C}H_3{}^{iPr}$).

Synthesis of [Ta($CH_2{}^tBu$)$_2$($CH{}^tBu$)(μ-$CH{}^tBu$)Au(IPr)] (3-Au). In the glovebox, complex **2-Au** (100 mg, 0.85 mmol) was dissolved in 3 mL of pentane within a 20 mL vial, and the mixture was left stirring overnight. Subsequently, the vial was gently opened to facilitate the gradual evaporation of pentane over an additional night, resulting in the formation of a yellow-orange crystalline solid. This solid was then promptly rinsed with approximately 1 mL of cold pentane (−40 °C), yielding **3-Au** in the form of small yellow crystals (40 mg, 40% yield). Do to fluxional dynamics occurring on the NMR time scale at room temperature, resulting in signal broadening that complicates their assignment, the solution NMR characterization of **3-Au** was conducted at 253 K. This lower temperature facilitated a more comprehensive and accurate signal assignment. ^1H NMR (500 MHz, toluene-d_8, 253 K) δ ppm 7.25 (t, $^3J_{1H-1H}$ = 7.8 Hz, 2H, 2 *para* C$\underline{H}^{Ar}$), 7.11−6.98 (m, 4H, 4 *meta* C$\underline{H}^{Ar}$), 6.28 (s, 1H, N−C$\underline{H}$═C$\underline{H}$−N), 2.83 (hept, $^3J_{1H-1H}$ = 7.2 Hz, 2H, 2 C$\underline{H}$(CH_3)$_2$), 2.67 (hept, $^3J_{1H-1H}$ = 7.2 Hz, 2H, 2 C$\underline{H}$(CH_3)$_2$), 2.19 (s, 1H, AuTaC$\underline{H}$C(CH_3)$_3$), 1.79 (s, 1H, TaC$\underline{H}$C(CH_3)$_3$), 1.75 (s, 9H, AuTaCHC($C\underline{H}_3$)$_3$), 1.56 (d, $^3J_{1H-1H}$ = 6.8 Hz, 6H, CH($C\underline{H}_3$)$_2$), 1.50−1.43 (m, 15H, TaCH$_2$C-($C\underline{H}_3$)$_3$ and CH($C\underline{H}_3$)$_2$), 1.34 (s, 9H, TaCH$_2$C($C\underline{H}_3$)$_3$), 1.12−1.05 (m, 21H, TaCHC($C\underline{H}_3$)$_3$, and 2 CH($C\underline{H}_3$)$_2$), 1.01 (d, $^2J_{1H-1H}$ = 13.4 Hz, 1H, TaC$\underline{H}_2$C(CH_3)$_3$), 0.66 (s, 2H, TaC$\underline{H}_2$C(CH_3)$_3$), −0.34 (d, $^2J_{1H-1H}$ = 13.4 Hz, 1H, TaC$\underline{H}_2$C(CH_3)$_3$). $^{13}C\{^1H\}$-NMR (126 MHz, toluene-d_8, 253 K) δ ppm 229.51 (s, 1C, Ta$\underline{C}$HC(CH_3)$_3$), 202.23 (s, 1C, Au$\underline{C}^{NHC}$), 167.59 (s, 1C, AuTa$\underline{C}$HC(CH_3)$_3$), 145.00 (s, 2C, 2 $\underline{C}^{Ar}$*i*Pr), 144.78 (s, 2C, 2 $\underline{C}^{Ar}$*i*Pr), 134.60 (s, 2C, 2 $\underline{C}^{Ar}$N), 130.77 (s, 2C, 2 *para*C$\underline{H}^{Ar}$), 124.27 (s, 2C, 2 *meta*C$\underline{H}^{Ar}$), 124.09 (s, 2C, 2 *meta*C$\underline{H}^{Ar}$), 122.79 (s, 2C, *N*−$\underline{C}$H═$\underline{C}$H−N), 103.27 (s, 1C, 1 Ta$\underline{C}H_2$C(CH_3)$_3$), 92.45 (s, 1C, 1 Ta$\underline{C}H_2$C(CH_3)$_3$), 46.83 (s, 1C, AuTaCH$\underline{C}$(CH_3)$_3$), 43.66 (s, 1C, TaCH$\underline{C}$(CH_3)$_3$), 38.15 (s, 3C, TaCHC($\underline{C}H_3$)$_3$), 35.38 (s, 3C, TaCH$_2$C($\underline{C}H_3$)$_3$), 35.06 (s, 3C, TaCH$_2$C($\underline{C}H_3$)$_3$), 34.94 (s, 3C, AuTaCHC($\underline{C}H_3$)$_3$), 34.39 (s, 1C, TaCH$_2\underline{C}$(CH_3)$_3$), 34.01 (s, 1C, TaCH$_2\underline{C}$(CH_3)$_3$), 28.65 (s, 4C, 4 $\underline{C}H^{iPr}$), 24.38 (s, 2C, 2 $\underline{C}H_3{}^{iPr}$), 24.18 (s, 2C, 2 $\underline{C}H_3{}^{iPr}$), 24.01 (s, 2C, 2 $\underline{C}H^{iPr}$), 23.91 (s, 2C, 2 $\underline{C}H_3{}^{iPr}$). Anal. calcd for $C_{47}H_{78}AuN_2Ta$: C, 53.81; H, 7.49; N, 2.67. Found: C, 53.83; H, 7.51; N, 2.63.

Synthesis of [Cu(C(CO)^{t}Bu)(IPr)] (4-Cu). A solution of **2-Cu** (100 mg, 0.11 mmol) in pentane (5 mL) was cooled to −80 °C with an acetone/liquid nitrogen bath and then exposed to a CO_2 atmosphere (0.78 bar, 70.5 mL headspace, 0.22 mmol, 2 equiv). The mixture was stirred for 10 min at this temperature and then for 1 h at room temperature. The orange color of the starting product disappears, and a white precipitate was formed, which was then filtered, washed with pentane (3 × 2 mL), and dried in vacuum to give product **4** as a white solid (29 mg, 48% yield). Crystals of **4** suitable for X-ray diffraction studies were obtained by slow recrystallization of a saturated toluene solution of **4** at −40 °C over a period of 16 h. ^1H NMR (500 MHz, C_6D_6, 298 K) δ ppm 7.21 (t, $^3J_{1H-1H}$ = 7.8 Hz, 2H, 2 *para* C$\underline{H}^{Ar}$), 7.07 (d, $^3J_{1H-1H}$ = 7.8 Hz, 4H, 4 *meta* C$\underline{H}^{Ar}$), 6.27 (s, 2H, N−C$\underline{H}$═C$\underline{H}$-N), 2.60 (*hept*, $^3J_{1H-1H}$ = 6.7 Hz, 4H, 4 C$\underline{H}$(CH_3)$_2$), 1.44 (d, $^3J_{1H-1H}$ = 6.9 Hz, 12H, 2 CH($C\underline{H}_3$)$_2$), 1.15 (s, 9H, CuC(CO)C($C\underline{H}_3$)$_3$), 1.08 (d, $^3J_{1H-1H}$ = 6.9 Hz, 12H, 2 CH($C\underline{H}_3$)$_2$). $^{13}C\{^1H\}$-NMR (126 MHz, C_6D_6, 298 K) δ ppm 183.83 (s, 1C, Cu$\underline{C}^{NHC}$), 169.89 (s, 1C, CuC($\underline{C}$O)C(CH_3)$_3$), 145.80 (s, 4C, 4 $\underline{C}^{Ar}$*i*Pr), 135.11 (s, 2C, 2 $\underline{C}^{Ar}$N), 130.64 (s, 2C, 2 *para*C$\underline{H}^{Ar}$), 124.28 (s, 4C, 4 *meta*C$\underline{H}^{Ar}$), 122.25 (s, 2C, *N*−$\underline{C}$H═$\underline{C}$H−N), 36.67 (s, 3C, CuC(CO)C($\underline{C}H_3$)$_3$), 32.19 (s, 1C, CuC(CO)$\underline{C}$(CH_3)$_3$), 29.04 (s, 4C, 4 $\underline{C}H^{iPr}$), 24.91 (s, 4C, 4 $\underline{C}H_3{}^{iPr}$), 24.39 (s, 1C, Cu$\underline{C}$(CO)C(CH_3)$_3$), 23.94 (s, 4C, 4 $\underline{C}H_3{}^{iPr}$). DRIFT (293 K, cm^{-1}) ν = 3163 (s), 3138 (s), 2961 (s), 2891 (s), 2868 (s), 2012 (s, $\nu_{CC=O}$), 1469 (s), 1404 (s), 1384 (s), 1364 (s), 1355 (s), 1327 (s), 1211 (s), 1179 (s), 1060 (s), 946 (s). Anal. calcd for $C_{33}H_{45}CuN_2O$: C, 72.16; H, 8.26; N, 5.10. Found: C, 70.00; H, 8.06; N, 5.01.

Synthesis of [Ag(C(CO)^{t}Bu)(IPr)] (4-Ag). A solution of **2-Ag** (100 mg, 0.104 mmol) in pentane (5 mL) was cooled to −80 °C and then exposed to a CO_2 atmosphere (73 mbar, 70.5 mL headspace, 0.208 mmol, 2 equiv). The mixture was stirred for 10 min at this temperature and then for 1 h at room temperature. The orange color of the starting product disappears, and a white precipitate was formed, which was then filtered, washed with pentane (3 × 2 mL), and dried in vacuum to give product **4-Ag** as a white solid (29 mg, 49% yield). ^1H NMR (500 MHz, THF-d_8, 298 K) δ ppm 7.58 (d, $^3J_{1H-1H}$ = 1.1 Hz, 2H, N−C$\underline{H}$═C$\underline{H}$−N), 7.47 (t, $^3J_{1H-1H}$ = 7.8 Hz, 2H, 2 *para* C$\underline{H}^{Ar}$), 7.34 (d, $^3J_{1H-1H}$ = 7.8 Hz, 4H, 4 *meta* C$\underline{H}^{Ar}$), 2.65 (*hept*, $^3J_{1H-1H}$ = 6.8 Hz, 4H, 4 C$\underline{H}$(CH_3)$_2$), 1.30 (d, $^3J_{1H-1H}$ = 6.9 Hz, 12H, 2 CH($C\underline{H}_3$)$_2$), 1.23 (d, $^3J_{1H-1H}$ = 6.9 Hz, 12H, 2 CH($C\underline{H}_3$)$_2$). 0.73 (s, 9H, AgC(CO)C($C\underline{H}_3$)$_3$). ^1H NMR (300 MHz, C_6D_6, 298 K) δ ppm 7.24−7.14 (m, 2H, 2 *para* C$\underline{H}^{Ar}$), 7.04 (d, $^3J_{1H-1H}$ = 7.7 Hz, 4H, 4 *meta* C$\underline{H}^{Ar}$), 6.31 (s, 2H, N−C$\underline{H}$═C$\underline{H}$-N), 2.53 (*hept*, $^3J_{1H-1H}$ = 6.8 Hz, 4H, 4 C$\underline{H}$(CH_3)$_2$), 1.37 (d, $^3J_{1H-1H}$ = 6.8 Hz, 12H, 2 CH($C\underline{H}_3$)$_2$), 1.21 (s, 9H, AgC(CO)C($C\underline{H}_3$)$_3$), 1.05 (d, $^3J_{1H-1H}$ = 6.8 Hz, 12H, 2 CH($C\underline{H}_3$)$_2$). $^{13}C\{^1H\}$-NMR (126 MHz, THF-d_8, 298 K) δ ppm 189.20 (d, $^1J_{13C-109Ag}$ = 192.2 Hz and d, $^1J_{13C-107Ag}$ = 167.5 Hz, 1C, Ag$\underline{C}^{NHC}$), 169.38 (d, $^2J_{13C-109Ag}$ = $^2J_{13C-107Ag}$ = 3.3 Hz, 1C, AgC($\underline{C}$O)C(CH_3)$_3$), 146.83 (s, 4C, 4 $\underline{C}^{Ar}$*i*Pr), 136.50 (s, 2C, 2 $\underline{C}^{Ar}$N), 131.12 (s, 2C, 2 *para*$\underline{C}H^{Ar}$), 124.95 (s, 4C, 4 *meta*$\underline{C}H^{Ar}$), 124.79 (d, $^3J_{13C-109Ag}$ = $^3J_{13C-107Ag}$ = 5.2 Hz, 2C, *N*−$\underline{C}$H═$\underline{C}$H−N),

https://doi.org/10.1021/jacs.4c02172
J. Am. Chem. Soc. 2024, 146, 18306−18319

37.17 (d, $^{3}J_{13C-109Ag}$ = $^{3}J_{13C-107Ag}$ = 3.9, 3C, AgC(CO)C($\underline{C}H_3$)$_3$), 32.20 (d, $^{2}J_{13C-109Ag}$ = $^{2}J_{13C-107Ag}$ = 6.2, 1C, AgC(CO)$\underline{C}$(CH$_3$)$_3$), 29.75 (s, 4C, 4 $\underline{C}H^{iPr}$), 25.12 (s, 4C, 4 $\underline{C}H_3^{iPr}$), 24.33 (s, 4C, 4 $\underline{C}H_3^{iPr}$), 23.70 (d, $^{1}J_{13C-109Ag}$ = 121.78 Hz and d, $^{1}J_{13C-107Ag}$ = 104.62 Hz 1C, Ag$\underline{C}$(CO)C(CH$_3$)$_3$). DRIFT (293 K, cm^{-1}) ν = 3165 (s), 3141 (s), 2962 (s), 2890 (s), 2868 (s), 2016 (s, $\nu_{CC=O}$), 1593 (s), 1469 (s), 1456 (s), 1406 (s), 1384 (s), 1363 (s), 1355 (s), 1328 (s), 1211 (s), 1178 (s), 1115 (s), 1102 (s), 1056 (s), 936 (s). Anal. calcd for $C_{33}H_{45}AgN_2O$: C, 66.77; H, 7.64; N, 4.72. Found: C, 66.33; H, 7.60; N, 4.55.

Synthesis of [Au(C(CO)^{t}Bu)(IPr)] (4-Au). A solution of **2-Au** (100 mg, 0.095 mmol) in pentane (5 mL) was cooled to −80 °C and then exposed to a CO_2 atmosphere (67 mbar, 70.5 mL headspace, 0.20 mmol, 2 equiv). The mixture was stirred for 10 min at this temperature and then for 1 h at room temperature. The orange/brown color of the starting product disappears, and a white precipitate was formed, which was then filtered, washed with pentane (3 × 2 mL), and dried in vacuum to give a white solid (69 mg). The yield of the reaction was estimated by ^{1}H NMR from this solid using durene as an internal standard (77%), since one unidentified impurity cocrystallized with the final product. Unfortunately, despite numerous attempts, we failed to remove this impurity by fractional recrystallizations. ^{1}H NMR (500 MHz, THF-d_8, 298 K) δ ppm 7.53 (s, 2H, N−C$\underline{H}$═C$\underline{H}$−N), 7.45 (t, $^{3}J_{1H-1H}$ = 7.8 Hz, 2H, 2 *para* C$\underline{H}^{Ar}$), 7.31 (d, = 7.8 Hz, 4H, 4 *meta* C$\underline{H}^{Ar}$), 2.68 (*hept*, $^{3}J_{1H-1H}$ = 6.9 Hz, 4H, 4 C$\underline{H}$(CH$_3$)$_2$), 1.36 (d, $^{3}J_{1H-1H}$ = 6.9 Hz, 12H, 2 CH(C$\underline{H}_3$)$_2$), 1.22 (d, $^{3}J_{1H-1H}$ = 6.9 Hz, 12H, 2 CH(C$\underline{H}_3$)$_2$), 0.72 (s, 9H, AuC(CO)C(C$\underline{H}_3$)$_3$). ^{1}H NMR (300 MHz, C_6D_6, 298 K) δ ppm 7.26−7.11 (m, 2H, 2 *para* C$\underline{H}^{Ar}$), 7.05 (d, $^{3}J_{1H-1H}$ = 7.7 Hz, 4H, 4 *meta* C$\underline{H}^{Ar}$), 6.26 (s, 2H, N−C$\underline{H}$═C$\underline{H}$-N), 2.60 (*hept*, $^{3}J_{1H-1H}$ = 6.7 Hz, 4H, 4 C$\underline{H}$(CH$_3$)$_2$), 1.48 (d, $^{3}J_{1H-1H}$ = 6.8 Hz, 12H, 2 CH(C$\underline{H}_3$)$_2$), 1.16 (s, 9H, AuC(CO)C(C$\underline{H}_3$)$_3$), 1.07 (d, $^{3}J_{1H-1H}$ = 6.8 Hz, 12H, 2 CH(C$\underline{H}_3$)$_2$). ^{13}C{^{1}H}-NMR (126 MHz, THF-d_8, 298 K) δ ppm 193.39 (s, 1C, Au$\underline{C}^{NHC}$), 181.19 (s, 1C, AuC($\underline{C}$O)C-(CH$_3$)$_3$), 146.84 (s, 4C, 4 $\underline{C}^{Ar}$*i*Pr), 136.11 (s, 2C, 2 $\underline{C}^{Ar}$N), 130.99 (s, 2C, 2 *para*$\underline{C}H^{Ar}$), 124.80 (s, 4C, 4 *meta*$\underline{C}H^{Ar}$), 124.30 (s, 2C, *N*−$\underline{C}$H═$\underline{C}$H−N), 39.71 (s, 1C, AuC(CO)$\underline{C}$(CH$_3$)$_3$), 36.45 (s, 3C, AuC(CO)C($\underline{C}$H$_3$)$_3$), 32.00 (s, 1C, Au$\underline{C}$(CO)C(CH$_3$)$_3$), 29.80 (s, 4C, 4 $\underline{C}H^{iPr}$), 24.84 (s, 4C, 4 $\underline{C}H_3^{iPr}$), 24.40 (s, 4C, 4 $\underline{C}H_3^{iPr}$). DRIFT (293 K, cm^{-1}) ν = 3166 (s), 3142 (s), 2960 (s), 2894 (s), 2867 (s), 2027 (s, $\nu_{CC=O}$), 1552 (s), 1470 (s), 1414 (s), 1384 (s), 1364 (s), 1357 (s), 1328 (s), 1315 (s), 1257 (s), 1232 (s), 1180 (s), 1117 (s), 1060 (s), 947 (s), 936 (s), 866 (s), 805 (s), 768 (s).

Reactivity of Compound 1 with CO_2. A solution of complex **1** (100 mg, 0.16 mmol) in pentane (5 mL) was exposed to a CO_2 atmosphere (114 mbar, 70.5 mL headspace, 0.33 mmol, 2 equiv). The mixture was stirred for 90 min. A yellow precipitate formed, which was then filtered, washed with pentane (3 × 2 mL), and dried under vacuum to yield a yellow pale powder (60 mg). This solid appeared to be insoluble in pentane (as well as in C_6D_6). It was subsequently analyzed by ^{1}H NMR in THF-d_8 (see Figure S64), revealing the formation of a mixture of unknown diamagnetic compounds. The supernatant solution was also evaporated under vacuum and analyzed by ^{1}H NMR, revealing the full consumption of complex **1** in this reaction (see Figure S65).

■ ASSOCIATED CONTENT

Supporting Information

The Supporting Information is available free of charge at https://pubs.acs.org/doi/10.1021/jacs.4c02172.

NMR and DRIFT spectra (Figures S1−S66); XRD, projection of the reciprocal space (Figures S67−S70); and computational data (Figures DFT-1−DFT-9); crystallographic parameters (Tables S1, S2); relative stability (Table S3) (PDF)

Accession Codes

CCDC 2310994−2310999 contain the supplementary crystallographic data for this paper. These data can be obtained free of charge via www.ccdc.cam.ac.uk/data_request/cif, or by emailing data_request@ccdc.cam.ac.uk, or by contacting The Cambridge Crystallographic Data Centre, 12 Union Road, Cambridge CB2 1EZ, UK; fax: +44 1223 336 033.

■ AUTHOR INFORMATION

Corresponding Author

Clément Camp − *Laboratory of Catalysis, Polymerization, Processes and Materials (CP2M UMR 5128), CNRS, Universite Claude Bernard Lyon 1, CPE-Lyon, Institut de Chimie de Lyon, Villeurbanne F-69616, France;* orcid.org/0000-0001-8528-0731; Email: clement.camp@univ-lyon1.fr

Authors

Abdelhak Lachguar − *Laboratory of Catalysis, Polymerization, Processes and Materials (CP2M UMR 5128), CNRS, Universite Claude Bernard Lyon 1, CPE-Lyon, Institut de Chimie de Lyon, Villeurbanne F-69616, France*

Iker Del Rosal − *CNRS, INSA, UPS, UMR 5215, LPCNO, Université de Toulouse, Toulouse F-31077, France;* orcid.org/0000-0001-6898-4550

Laurent Maron − *CNRS, INSA, UPS, UMR 5215, LPCNO, Université de Toulouse, Toulouse F-31077, France;* orcid.org/0000-0003-2653-8557

Erwann Jeanneau − *Centre de Diffractométrie Henri Longchambon, Université de Lyon, Villeurbanne 69100, France*

Laurent Veyre − *Laboratory of Catalysis, Polymerization, Processes and Materials (CP2M UMR 5128), CNRS, Universite Claude Bernard Lyon 1, CPE-Lyon, Institut de Chimie de Lyon, Villeurbanne F-69616, France*

Chloé Thieuleux − *Laboratory of Catalysis, Polymerization, Processes and Materials (CP2M UMR 5128), CNRS, Universite Claude Bernard Lyon 1, CPE-Lyon, Institut de Chimie de Lyon, Villeurbanne F-69616, France;* orcid.org/0000-0002-5436-2467

Complete contact information is available at: https://pubs.acs.org/10.1021/jacs.4c02172

Author Contributions

All authors have given approval to the final version of the manuscript.

Funding

Funded by the European Union (ERC, DUO 101 041 762). Views and opinions expressed are, however, those of the authors only and do not necessarily reflect those of the European Union or the European Research Council. Neither the European Union nor the granting authority can be held responsible for them. The computational work was performed using the HPC resources from CALMIP (Grant 2016-p0833).

Notes

The authors declare no competing financial interest.

this submission, in accordance with the grant's open access conditions.

■ ACKNOWLEDGMENTS

L. M. is a senior member of the "Institut Universitaire de France". Anne Baudouin and Emmanuel Chefdeville are acknowledged for their help in acquiring the NMR data.

■ REFERENCES

(1) Navarro, M.; Bourissou, D. π-Alkene/Alkyne and Carbene Complexes of Gold(I) Stabilized by Chelating Ligands. In *Advances in Organometallic Chemistry*; Academic Press, 2021; Vol. *76*, pp. 101144. DOI: .

(2) Mehara, J.; Watson, B. T.; Noonikara-Poyil, A.; Zacharias, A. O.; Roithová, J.; Rasika Dias, H. V. Binding Interactions in Copper, Silver and Gold π-Complexes. *Chem. - A Eur. J.* **2022**, *28* (13), No. e202103984.

(3) Navarro, M.; Toledo, A.; Mallet-Ladeira, S.; Sosa Carrizo, E. D.; Miqueu, K.; Bourissou, D. Versatility and Adaptative Behaviour of the P^N Chelating Ligand MeDalphos within Gold(I) π Complexes. *Chem. Sci.* **2020**, *11* (10), 2750−2758.

(4) Rodriguez, J.; Szalóki, G.; Sosa Carrizo, E. D.; Saffon-Merceron, N.; Miqueu, K.; Bourissou, D. Gold(III) π-Allyl Complexes. *Angew. Chemie Int. Ed.* **2020**, *59* (4), 1511−1515.

(5) Thompson, J. S.; Harlow, R. L.; Whitney, J. F. Copper(I)-Olefin Complexes. Support for the Proposed Role of Copper in the Ethylene Effect in Plants. *J. Am. Chem. Soc.* **1983**, *105* (11), 3522−3527.

(6) Dias, H. V. R.; Wu, J. Structurally Characterized Coinage-Metal−Ethylene Complexes. *Eur. J. Inorg. Chem* **2008**, *2008* (4), 509−522.

(7) Dias, H. V. R.; Lovely, C. J. Carbonyl and Olefin Adducts of Coinage Metals Supported by Poly(Pyrazolyl)Borate and Poly-(Pyrazoly)Alkane Ligands and Silver Mediated Atom Transfer Reactions. *Chem. Rev.* **2008**, *108* (8), 3223−3238.

(8) Wang, W.; Zhai, X. Y.; Zhao, L. Mechanistic Insights into Multisilver-Mediated Synergistic Activation of Terminal Alkynes. *Inorg. Chem.* **2023**, *62* (4), 1414−1422.

(9) Navarro, M.; Toledo, A.; Joost, M.; Amgoune, A.; Mallet-Ladeira, S.; Bourissou, D. π Complexes of P^P and P^N Chelated Gold(I). *Chem. Commun.* **2019**, *55* (55), 7974−7977.

(10) Motloch, P.; Jašík, J.; Roithová, J. Gold(I) and Silver(I) π-Complexes with Unsaturated Hydrocarbons. *Organometallics* **2021**, *40* (10), 1492−1502.

(11) Deolka, S.; Rivada-Wheelaghan, O.; Aristizábal, S. L.; Fayzullin, R. R.; Pal, S.; Nozaki, K.; Khaskin, E.; Khusnutdinova, J. R. Metal-Metal Cooperative Bond Activation by Heterobimetallic Alkyl, Aryl, and Acetylide PtII/CuIcomplexes. *Chem. Sci.* **2020**, *11* (21), 5494−5502.

(12) Zacharias, A. O.; Mao, J. X.; Nam, K.; Dias, H. V. R. Copper(I) and Silver(I) Chemistry of Vinyltrifluoroborate Supported by a Bis(Pyrazolyl)Methane Ligand. *Dalton Trans.* **2021**, *50* (22), 7621−7632.

(13) Noonikara-Poyil, A.; Cui, H.; Yakovenko, A. A.; Stephens, P. W.; Lin, R.-B.; Wang, B.; Chen, B.; Dias, H. V. R. A Molecular Compound for Highly Selective Purification of Ethylene. *Angew. Chem.* **2021**, *133* (52), 27390−27394.

(14) Chambrier, I.; Rocchigiani, L.; Hughes, D. L.; Budzelaar, P. M. H.; Bochmann, M. Thermally Stable Gold(III) Alkene and Alkyne Complexes: Synthesis, Structures, and Assessment of the Trans-Influence on Gold−Ligand Bond Enthalpies. *Chem. - Eur. J.* **2018**, *24* (44), 11467−11474.

(15) Rocchigiani, L.; Fernandez-Cestau, J.; Agonigi, G.; Chambrier, I.; Budzelaar, P. H. M.; Bochmann, M. Gold(III) Alkyne Complexes: Bonding and Reaction Pathways. *Angew. Chem., Int. Ed.* **2017**, *56* (44), 13861−13865.

(16) Langseth, E.; Scheuermann, M. L.; Balcells, D.; Kaminsky, W.; Goldberg, K. I.; Eisenstein, O.; Heyn, R. H.; Tilset, M. Generation and Structural Characterization of a Gold(III) Alkene Complex. *Angew. Chem., Int. Ed.* **2013**, *52* (6), 1660−1663.

(17) Savjani, N.; Roşca, D. A.; Schormann, M.; Bochmann, M. Gold(III) Olefin Complexes. *Angew. Chem., Int. Ed.* **2013**, *52* (3), 874−877.

(18) Praveen, C. Carbophilic Activation of π-Systems via Gold Coordination: Towards Regioselective Access of Intermolecular Addition Products. *Coord. Chem. Rev.* **2019**, *392*, 1−34.

(19) Tang, X.-T.; Yang, F.; Zhang, T.-T.; Liu, Y.-F.; Liu, S.-Y.; Su, T.-F.; Lv, D.-C.; Shen, W.-B. Recent Progress in N-Heterocyclic Carbene Gold-Catalyzed Reactions of Alkynes Involving Oxidation/Amination/Cycloaddition. *Catalysts* **2020**, *10* (3), 350.

(20) López-Carrillo, V.; Echavarren, A. M. Gold(I)-Catalyzed Intermolecular [2 + 2] Cycloaddition of Alkynes with Alkenes. *J. Am. Chem. Soc.* **2010**, *132* (27), 9292−9294.

(21) Zanini, M.; Cataffo, A.; Echavarren, A. M. Synthesis of Cyclobutanones by Gold(I)-Catalyzed [2 + 2] Cycloaddition of Ynol Ethers with Alkenes. *Org. Lett.* **2021**, *23* (22), 8989−8993.

(22) Rigoulet, M.; Thillaye du Boullay, O.; Amgoune, A.; Bourissou, D. Gold(I)/Gold(III) Catalysis That Merges Oxidative Addition and π-Alkene Activation. *Angew. Chem., Int. Ed.* **2020**, *59* (38), 16625−16630.

(23) Hashmi, A. S. K.; Lauterbach, T.; Nösel, P.; Vilhelmsen, M. H.; Rudolph, M.; Rominger, F. Dual Gold Catalysis: σ,π-Propyne Acetylide and Hydroxyl-Bridged Digold Complexes as Easy-to-Prepare and Easy-to-Handle Precatalysts. *Chem. - A Eur. J.* **2013**, *19* (3), 1058−1065.

(24) Nunes Dos Santos Comprido, L.; Klein, J. E. M. N.; Knizia, G.; Kästner, J.; Hashmi, A. S. K. Gold(I) Vinylidene Complexes as Reactive Intermediates and Their Tendency to π-Backbond. *Chem. - A Eur. J.* **2016**, *22* (9), 2892−2895.

(25) Hashmi, A. S. K. Gold-Catalyzed Organic Reactions. *Chem. Rev.* **2007**, *107*, 3180−3211.

(26) Fürstner, A. From Understanding to Prediction: Gold- and Platinum-Based Π-Acid Catalysis for Target Oriented Synthesis. *Acc. Chem. Res.* **2014**, *47* (3), 925−938.

(27) Jones, A. C. Gold π-Complexes as Model Intermediates in Gold Catalysis. *Top. Curr. Chem.* **2014**, *357*, 133−166.

(28) Rodriguez, J.; Vesseur, D.; Tabey, A.; Mallet-Ladeira, S.; Miqueu, K.; Bourissou, D. Au(I)/Au(III) Catalytic Allylation Involving π-Allyl Au(III) Complexes. *ACS Catal.* **2022**, *12* (2), 993−1003.

(29) Praveen, C.; Szafert, S. Homogeneous Gold Catalysis for Regioselective Carbocyclization of Alkynyl Precursors. *ChemPluschem* **2023**, *88* (7), No. e202300202.

(30) Hashmi, A. S. K.; Hutchings, G. J. Gold Catalysis. *Angew. Chem., Int. Ed.* **2006**, *45* (47), 7896−7936.

(31) Bai, Y.-B.; Luo, Z.; Wang, Y.; Gao, J.-M.; Zhang, L. Au-Catalyzed Intermolecular [2 + 2] Cycloadditions between Chloroalkynes and Unactivated Alkenes. *J. Am. Chem. Soc.* **2018**, *140* (17), 5860−5865.

(32) De Orbe, M. E.; Amenós, L.; Kirillova, M. S.; Wang, Y.; López-Carrillo, V.; Maseras, F.; Echavarren, A. M. Cyclobutene vs 1,3-Diene Formation in the Gold-Catalyzed Reaction of Alkynes with Alkenes: The Complete Mechanistic Picture. *J. Am. Chem. Soc.* **2017**, *139* (30), 10302−10311.

(33) Sweis, R. F.; Schramm, M. P.; Kozmin, S. A. Silver-Catalyzed [2 + 2] Cycloadditions of Siloxy Alkynes. *J. Am. Chem. Soc.* **2004**, *126* (24), 7442−7443.

(34) Braunschweig, H.; Radacki, K.; Shang, R. Side-on Coordination of Boryl and Borylene Complexes to Cationic Coinage Metal Fragments. *Chem. Sci.* **2015**, *6* (5), 2989−2996.

(35) Carriedo, G. A.; Riera, V.; Sánchez, G.; Solans, X. Synthesis of New Heteronuclear Complexes with Bridging Carbyne Ligands between Tungsten and Gold. X-Ray Crystal Structure of [AuW(μ-CC6H4Me-4)(CO)2(Bipy)(C6F5)Br]. *J. Chem. Soc., Dalton Trans.* **1988**, *7*, 1957−1962.

(36) Onn, C. S.; Hill, A. F.; Olding, A. Metal Coordination of Phosphoniocarbynes. *Dalton Trans.* **2020**, *49* (36), 12731−12741.

(37) Manzano, R. A.; Hill, A. F. Fluorocarbyne Complexes via Electrophilic Fluorination of Carbido Ligands. *Chem. Sci.* **2023**, *14* (14), 3776−3781.
(38) Clark, G. R.; Cochrane, C. M.; Roper, W. R.; Wright, L. J. The Interaction of an Osmium-Carbon Triple Bond with Copper(I), Silver(I) and Gold(I) to Give Mixed Dimetallocyclopropene Species and the Structures of Os(AgCl) (CR) Cl(CO) (PPh3)2. *J. Organomet. Chem.* **1980**, *199* (2), C35−C38.
(39) Zhou, X.; Li, Y.; Shao, Y.; Hua, Y.; Zhang, H.; Lin, Y. M.; Xia, H. Reactions of Cyclic Osmacarbyne with Coinage Metal Complexes. *Organometallics* **2018**, *37* (11), 1788−1794.
(40) Borren, E. S.; Hill, A. F.; Shang, R.; Sharma, M.; Willis, A. C. A Golden Ring: Molecular Gold Carbido Complexes. *J. Am. Chem. Soc.* **2013**, *135* (13), 4942−4945.
(41) Frogley, B. J.; Hill, A. F.; Onn, C. S. Auriferous Alkynylselenolatoalkylidynes. *Dalton Trans.* **2019**, *48* (31), 11715−11723.
(42) Phillips, N. A.; Kong, R. Y.; White, A. J. P.; Crimmin, M. R. Group 11 Borataalkene Complexes: Models for Alkene Activation. *Angew. Chemie Int. Ed.* **2021**, *60* (21), 12013−12019.
(43) Suzuki, A.; Wu, L.; Lin, Z.; Yamashita, M. Isomerization of a Cis-(2-Borylalkenyl)Gold Complex via a Retro-1,2-Metalate Shift: Cleavage of a C−C/C−Si Bond Trans to a C−Au Bond. *Angew. Chem., Int. Ed.* **2021**, *60* (38), 21007−21013.
(44) Wisofsky, G. K.; Rojales, K.; Su, X.; Bartholome, T. A.; Molino, A.; Kaur, A.; Wilson, D. J. D.; Dutton, J. L.; Martin, C. D. Ligation of Boratabenzene and 9-Borataphenanthrene to Coinage Metals. *Inorg. Chem.* **2021**, *60* (24), 18981−18989.
(45) Chen, C.; Daniliuc, C. G.; Kehr, G.; Erker, G. Bora-Alkenes: Metal Coordination and Reactions with BH-Boranes. *Chem. - Eur. J.* **2023**, *29* (41), No. e202301044.
(46) Frogley, B. J.; Hill, A. F.; Watson, L. J. New Binding Modes for CSe: Coinage Metal Coordination to a Tungsten Selenocarbonyl Complex. *Dalton Trans* **2019**, *48* (33), 12598−12606.
(47) Burt, L. K.; Dewhurst, R. D.; Hill, A. F.; Kong, R. Y.; Nahon, E. E.; Onn, C. S. Heterobimetallic M2-Halocarbyne Complexes. *Dalton Trans.* **2022**, *51* (32), 12080−12099.
(48) Zhuo, Q.; Zhang, H.; Hua, Y.; Kang, H.; Zhou, X.; Lin, X.; Chen, Z.; Lin, J.; Zhuo, K.; Xia, H. Constraint of a Ruthenium-Carbon Triple Bond to a Five-Membered Ring. *Sci. Adv.* **2018**, *4* (6), 336−358.
(49) Schrock, R. R. High Oxidation State Multiple Metal-Carbon Bonds. *Chem. Rev.* **2002**, *102* (1), 145−179.
(50) Ehrhorn, H.; Tamm, M. Well-Defined Alkyne Metathesis Catalysts: Developments and Recent Applications. *Chem. - Eur. J.* **2019**, *25* (13), 3190−3208.
(51) Fürstner, A.; Davies, P. W. Alkyne Metathesis. *Chem. Commun.* **2005**, *18*, 2307−2320.
(52) Guggenberger, L. J.; Schrock, R. R. A Tantalum Carbyne Complex. *J. Am. Chem. Soc.* **1975**, *97* (10), 2935.
(53) Rietveld, M. H. P.; Lohner, P.; Nijkamp, M. G.; Grove, D. M.; Veldman, N.; Spek, A. L.; Pfeffer, M.; Van Koten, G. A Novel Synthetic Route to Tantalum-Zinc Neophylidyne Complexes Stabilized by Ortho-Chelating Arylamine Ligands; the X-Ray Structure of [TaCl2(μ-C6H4CH2NMe2−2)(μ-CCMe2 Ph)ZnCl-(THF)]. *Chem. - Eur. J.* **1997**, *3* (5), 817−822.
(54) Gal, A. W.; Van Der Heijden, H. Synthesis and X-Ray Crystal Structure of the Trimetallic Neopentylidyne Complex [{Cl2-(MeOCH2CH2OMe)Ta(μ-CCMe 3)}2Zn(μ-Cl)2]. *J. Chem. Soc., Chem. Commun.* **1983**, *8*, 420−422.
(55) Abbenhuis, H. C. L.; Feiken, N.; Haarman, H. F.; Grove, D. M.; Horn, E.; Spek, A. L.; Pfeffer, M.; van Koten, G. A Bimetallic Tantalum-Zinc Complex with an Ancillary Aryldiamine Ligand as Precursor for a Reactive Alkylidyne Species: Alkylidyne-Mediated C-H Activation and a Palladium-Mediated Alkylidyne Functionalization. *Organometallics* **1993**, *12* (6), 2227−2235.
(56) Lohner, P.; Fischer, J.; Pfeffer, M. Synthesis and Reactivity of Early-Late Heterobimetallic Complexes Displaying a H2-Tantalum-Alkylidene to Palladium Interaction. *Inorg. Chim. Acta* **2002**, *330* (1), 220−228.
(57) Lachguar, A.; Pichugov, A. V.; Neumann, T.; Dubrawski, Z.; Camp, C. Cooperative Activation of Carbon-Hydrogen Bonds by Heterobimetallic Systems. *Dalton Trans.* **2024**, *53*, 1393−1409.
(58) Wei, R.; Wang, X. F.; Hu, C.; Liu, L. L. Synthesis and Reactivity of Copper Carbyne Anion Complexes. *Nat. Synth.* **2023**, *2* (4), 357−363.
(59) Hu, C.; Wang, X. F.; Wei, R.; Hu, C.; Ruiz, D. A.; Chang, X. Y.; Liu, L. L. Crystalline Monometal-Substituted Free Carbenes. *Chem* **2022**, *8* (8), 2278−2289.
(60) Alvarez, M. A.; García, M. E.; García-Vivó, D.; Martínez, M. E.; Ruiz, M. A. Binuclear Carbyne and Ketenyl Derivatives of the Alkyl-Bridged Complexes [Mo2(H5-C5H5) 2(μ-CH2R)(μ-PCy2)(CO)2] (R = H, Ph). *Organometallics* **2011**, *30* (8), 2189−2199.
(61) Wei, R.; Wang, X. F.; Ruiz, D. A.; Liu, L. L. Stable Ketenyl Anions via Ligand Exchange at an Anionic Carbon as Powerful Synthons**. *Angew. Chem., Int. Ed.* **2023**, *62* (15), No. e202219211.
(62) Jörges, M.; Krischer, F.; Gessner, V. H. Transition Metal−Free Ketene Formation from Carbon Monoxide through Isolable Ketenyl Anions. *Science* **2022**, *378* (6626), 1331−1336.
(63) Bailey, G. A.; Agapie, T. Terminal Mo Carbide and Carbyne Reactivity: H2Cleavage, B-C Bond Activation, and C-C Coupling. *Organometallics* **2021**, *40* (16), 2881−2887.
(64) Timmermann, C.; Thiem, P.; Wanitschke, D.; Hüttenschmidt, M.; Romischke, J.; Villinger, A.; Seidel, W. W. Migratory Insertion of Isocyanide into a Ketenyl-Tungsten Bond as Key Step in Cyclization Reactions. *Chem. Sci.* **2021**, *13* (1), 123−132.
(65) Xu, M.; Wang, T.; Qu, Z. W.; Grimme, S.; Stephan, D. W. Reactions of a Dilithiomethane with CO and N2O: An Avenue to an Anionic Ketene and a Hexafunctionalized Benzene. *Angew. Chem., Int. Ed.* **2021**, *60* (48), 25281−25285.
(66) Buss, J. A.; Bailey, G. A.; Oppenheim, J.; Vandervelde, D. G.; Goddard, W. A.; Agapie, T. CO Coupling Chemistry of a Terminal Mo Carbide: Sequential Addition of Proton, Hydride, and CO Releases Ethenone. *J. Am. Chem. Soc.* **2019**, *141* (39), 15664−15674.
(67) Santoro, S.; Himo, F. Mechanism of the Kinugasa Reaction Revisited. *J. Org. Chem.* **2021**, *86* (15), 10665−10671.
(68) Malig, T. C.; Yu, D.; Hein, J. E. A Revised Mechanism for the Kinugasa Reaction. *J. Am. Chem. Soc.* **2018**, *140* (29), 9167−9173.
(69) Torelli, A.; Choi, E. S.; Dupeux, A.; Perner, M. N.; Lautens, M. Stereoselective Kinugasa/Aldol Cyclization: Synthesis of Enantioenriched Spirocyclic β-Lactams. *Org. Lett.* **2023**, *25* (47), 8520−8525.
(70) Wang, H.; Jiang, L.; Liang, H.; Fan, H. Mechanism of Silver-Catalyzed[2 + 2] Cycloaddition between Siloxy-Alkynes and Carbonyl Compound: A Silylium Ion Migration Approach. *Chin. J. Org. Chem.* **2021**, *41* (11), 4327−4337.
(71) Srivastava, R.; Quadrelli, E. A.; Camp, C. Lability of Ta-NHC Adducts as a Synthetic Route towards Heterobimetallic Ta/Rh Complexes. *Dalton Trans.* **2020**, *49* (10), 3120−3128.
(72) Lassalle, S.; Petit, J.; Falconer, R. L.; Hérault, V.; Jeanneau, E.; Thieuleux, C.; Camp, C. Reactivity of Tantalum/Iridium and Hafnium/Iridium Alkyl Hydrides with Alkyl Lithium Reagents: Nucleophilic Addition, Alpha-H Abstraction, or Hydride Deprotonation? *Organometallics* **2022**, *41* (13), 1675−1687.
(73) Lassalle, S.; Jabbour, R.; Schiltz, P.; Berruyer, P.; Todorova, T. K.; Veyre, L.; Gajan, D.; Lesage, A.; Thieuleux, C.; Camp, C. Metal−Metal Synergy in Well-Defined Surface Tantalum−Iridium Heterobimetallic Catalysts for H/D Exchange Reactions. *J. Am. Chem. Soc.* **2019**, *141* (49), 19321−19335.
(74) Srivastava, R.; Moneuse, R.; Petit, J.; Pavard, P.-A.-A.; Dardun, V.; Rivat, M.; Schiltz, P.; Solari, M.; Jeanneau, E.; Veyre, L.; et al.etal. Early/Late Heterobimetallic Tantalum/Rhodium Species Assembled Through a Novel Bifunctional NHC-OH Ligand. *Chem. - Eur. J.* **2018**, *24* (17), 4361−4370.
(75) Lassalle, S.; Jabbour, R.; Del Rosal, I.; Maron, L.; Fonda, E.; Veyre, L.; Gajan, D.; Lesage, A.; Thieuleux, C.; Camp, C. Stepwise Construction of Silica-Supported Tantalum/Iridium Heteropolyme-

tallic Catalysts Using Surface Organometallic Chemistry. *J. Catal.* **2020**, *392*, 287−301.
(76) Camp, C.; Toniolo, D.; Andrez, J.; Pécaut, J.; Mazzanti, M. A Versatile Route to Homo- and Hetero-Bimetallic 5f-5f and 3d-5f Complexes Supported by a Redox Active Ligand Framework. *Dalton Trans.* **2017**, *46* (34), 11145.
(77) Banerjee, S.; Karunananda, M. K.; Bagherzadeh, S.; Jayarathne, U.; Parmelee, S. R.; Waldhart, G. W.; Mankad, N. P. Synthesis and Characterization of Heterobimetallic Complexes with Direct Cu-m Bonds (m = Cr, Mn, Co, Mo, Ru, w) Supported by N-Heterocyclic Carbene Ligands: A Toolkit for Catalytic Reaction Discovery. *Inorg. Chem.* **2014**, *53* (20), 11307−11315.
(78) Ye, C. Z.; Del Rosal, I.; Boreen, M. A.; Ouellette, E. T.; Russo, D. R.; Maron, L.; Arnold, J.; Camp, C. A Versatile Strategy for the Formation of Hydride-Bridged Actinide-Iridium Multimetallics. *Chem. Sci.* **2023**, *14* (4), 861−868.
(79) Gordon, C. P.; Raynaud, C.; Andersen, R. A.; Copéret, C.; Eisenstein, O. Carbon-13 NMR Chemical Shift: A Descriptor for Electronic Structure and Reactivity of Organometallic Compounds. *Acc. Chem. Res.* **2019**, *52* (8), 2278−2289.
(80) Fortman, G. C.; Slawin, A. M. Z.; Nolan, S. P. A Versatile Cuprous Synthon: [Cu(IPr)(OH)] (IPr = 1,3 Bis-(Diisopropylphenyl)Imidazol-2-Ylidene). *Organometallics* **2010**, *29* (17), 3966−3972.
(81) McLain, S. J.; Wood, C. D.; Messerle, L. W.; Schrock, R. R.; Hollander, F. J.; Youngs, W. J.; Churchill, M. R. Multiple Metal-Carbon Bonds. 10.1 Thermally Stable Tantalum Alkylidyne Complexes and the Crystal Structure of Ta(η-C5Me5)(CPh)(PMe3)-2Cl. *J. Am. Chem. Soc.* **1978**, *100* (18), 5962−5964.
(82) Fanwick, P. E.; Ogilvy, A. E.; Rothwell, I. P. Synthesis and Spectroscopic Properties of Tantalum 1/4-Alkylldyne Compounds Containing Bulky Aryloxide Ligands: X-Ray Structures of The Asymmetric Derivatives (Me2SiCH2)2ta(1/4-CSiMe3)2Ta-(Ch2SiMe3)(OAr-2,6-Ph2) and (Me2SiCH2)2Ta(CH-CSiMe3)-2Ta(OAr-2,6-t-Bu2)2(. *Organometallics* **1987**, *6* (1), 73−80.
(83) Churchill, M. R.; Holl, F. J. Crystal and molecular structure of a tantalum-alkylidene complex, bis(.eta.5-cyclopentadienyl)chloro-(neopentylidene)tantalum. *Inorg. Chem.* **1978**, *17* (7), 1957−1962.
(84) Schultz, A. J.; Williams, J. M.; Schröck, R. R.; Rupprecht, G. A.; Fellmann, J. D. Interaction of Hydrogen and Hydrocarbons with Transition Metals. Neutron Diffraction Evidence for an Activated Carbon-Hydrogen Bond in an Electron-Deficient Tantalum-Neopentylidene Complex. *J. Am. Chem. Soc.* **1979**, *101* (6), 1593−1595.
(85) Abbenhuis, H. C. L.; Feiken, N.; Grove, D. M.; Jastrzebski, J. T. B. H.; Kooijman, H.; van der Sluis, P.; Smeets, W. J. J.; Spek, A. L.; van Koten, G. Use of an Aryldiamine Pincer Ligand in the Study of Tantalum Alkylidene-Centered Reactivity: Tantalum-Mediated Alkene Synthesis via Reductive Rearrangements and Wittig-Type Reactions. *J. Am. Chem. Soc.* **1992**, *114* (25), 9773−9781.
(86) Jayarathne, U.; Mazzacano, T. J.; Bagherzadeh, S.; Mankad, N. P. Heterobimetallic Complexes with Polar, Unsupported Cu-Fe and Zn-Fe Bonds Stabilized by N-Heterocyclic Carbenes. *Organometallics* **2013**, *32* (14), 3986−3992.
(87) Bakhmutov, V. I.; Vorontsov, E. V.; Bakhmutova, E. V.; Boni, G.; Moise, C. Tantalum-Gold and Tantalum-Copper Trihydride Complexes Cp'2TaH3MPPh3[PF6] (Cp' = C5H4C(CH3)3). Structure Determination From1H T1 Relaxation Studies. *Inorg. Chem.* **1999**, *38* (6), 1121−1125.
(88) Pätow, R.; Isaac, I. Syntheses and Crystal Structures of Novel Heterobimetallic Tantalum Coin MetalChalcogenido Clusters. *Zeitschrift für Anorg. Und Allg. Chemie* **2002**, *628*, 1279−1288.
(89) Zhang, W. Q.; Morgan, H. W. T.; Shu, C. C.; McGrady, J. E.; Sun, Z. M. Synthesis and Characterization of Ternary Clusters Containing the [As16]10-Anion, [MM′As16]4-(M = Nb or Ta; M′= Cu or Ag). *Inorg. Chem.* **2022**, *61* (10), 4421−4427.
(90) Maiola, M. L.; Buss, J. A. Accessing Ta/Cu Architectures via Metal-Metal Salt Metatheses: Heterobimetallic C−H Bond Activation Affords μ-Hydrides. *Angew. Chem., Int. Ed.* **2023**, *62*, No. e202311721.
(91) Pauling, L. Atomic Radii and Interatomic Distances in Metals. *J. Am. Chem. Soc.* **1947**, *69* (3), 542−553.
(92) Cordero, B.; Gómez, V.; Platero-Prats, A. E.; Revés, M.; Echeverría, J.; Cremades, E.; Barragán, F.; Alvarez, S.; et al. Covalent Radii Revisited. *Dalton Trans.* **2008**, *44* (21), 2832.
(93) de Frémont, P.; Scott, N. M.; Stevens, E. D.; Ramnial, T.; Lightbody, O. C.; Macdonald, C. L. B. B.; Clyburne, J. A. C. C.; Abernethy, C. D.; Nolan, S. P. Synthesis of Well-Defined N-Heterocyclic Carbene Silver(I) Complexes. *Organometallics* **2005**, *24* (26), 6301−6309.
(94) Tzouras, N. V.; Saab, M.; Janssens, W.; Cauwenbergh, T.; Van Hecke, K.; Nahra, F.; Nolan, S. P. Simple Synthetic Routes to N-Heterocyclic Carbene Gold(I)−Aryl Complexes: Expanded Scope and Reactivity. *Chem. - Eur. J.* **2020**, *26* (24), 5541−5551.
(95) Chakarawet, K.; Davis-Gilbert, Z. W.; Harstad, S. R.; Young, V. G.; Long, J. R.; Ellis, J. E. Ta(CNDipp)6: An Isocyanide Analogue of Hexacarbonyltantalum(0). *Angew. Chem., Int. Ed.* **2017**, *56* (35), 10577−10581.
(96) Xue, Z. L.; Morton, L. A. Transition Metal Alkylidene Complexes. Pathways in Their Formation and Tautomerization between Bis-Alkylidenes and Alkyl Alkylidynes. *J. Organomet. Chem.* **2011**, *696* (25), 3924−3934.
(97) Morton, L. A.; Wang, R.; Yu, X.; Campana, C. F.; Guzei, I. A.; Yap, G. P. A.; Xue, Z. L. Tungsten Alkyl Alkylidyne and Bis-Alkylidene Complexes. Preparation and Kinetic and Thermodynamic Studies of Their Unusual Exchanges. *Organometallics* **2006**, *25* (2), 427−434.
(98) Morton, L. A.; Zhang, X. H.; Wang, R.; Lin, Z.; Wu, Y. D.; Xue, Z. L. An Unusual Exchange between Alkylidyne Alkyl and Bis(Alkylidene) Tungsten Complexes Promoted by Phosphine Coordination: Kinetic, Thermodynamic, and Theoretical Studies. *J. Am. Chem. Soc.* **2004**, *126* (33), 10208−10209.
(99) Dougan, B. A.; Xue, Z. L. Reaction of a Tungsten Alkylidyne Complex with a Chelating Diphosphine. α-Hydrogen Migration in the Intermediates and Formation of an Alkyl Alkylidene Alkylidyne Complex. *Organometallics* **2009**, *28* (5), 1295−1302.
(100) Berthoud, R.; Rendón, N.; Blanc, F.; Solans-Monfort, X.; Copéret, C.; Eisenstein, O. Metal Fragment Isomerisation upon Grafting a D2ML4 Perhydrocarbyl Os Complex on a Silica Surface: Origin and Consequence. *Dalton Trans.* **2009**, *30*, 5879−5886.
(101) Callens, E.; Abou-Hamad, E.; Riache, N.; Basset, J. M. Direct Observation of Supported W Bis-Methylidene from Supported W-Methyl/Methylidyne Species. *Chem. Commun.* **2014**, *50* (31), 3982−3985.
(102) Fellmann, J. D.; Rupprecht, G. A.; Wood, C. D.; Schrock, R. R. Multiple Metal-Carbon Bonds. 11.1 Bisneopentylidene Complexes of Niobium and Tantalum. *J. Am. Chem. Soc.* **1978**, *100* (18), 5964−5966.
(103) Giarrusso, C. P.; Zeil, D. V.; Blair, V. L. Catalytic Exploration of NHC-Ag(i)HMDS Complexes for the Hydroboration and Hydrosilylation of Carbonyl Compounds. *Dalton Trans.* **2023**, *52* (23), 7828−7835.
(104) Abbenhuis, H. C. L.; Rietveld, M. H. P.; Haarman, H. F.; Hogerheide, M. P.; Spek, A. L.; van Koten, G. Configurational Preferences and Alkylidene-Centered Reactivity of Tantalum Alkoxide Complexes Containing an Aryldiamine Spectator Ligand. *Organometallics* **1994**, *13* (8), 3259−3268.
(105) LaPointe, R. E.; Wolczanski, P. T.; Van Duyne, G. D. Tantalum Organometallics Containing Bulky Oxy Donors: Utilization of Tri-Tert-Butylsiloxide and 9-Oxytriptycene. *Organometallics* **1985**, *4* (10), 1810−1818.
(106) Schrock, R. R.; Fellmann, J. D. Multiple Metal-Carbon Bonds. 8. Preparation, Characterization, and Mechanism of Formation of the Tantalum and Niobium Neopentylidene Complexes, M(CH2CMe3)-3(CHCMe3). *J. Am. Chem. Soc.* **1978**, *100* (11), 3359−3370.
(107) Chabanas, M.; Quadrelli, E. A.; Fenet, B.; Copéret, C.; Thivolle-Cazat, J.; Basset, J.-M.; Lesage, A.; Emsley, L. Molecular Insight Into Surface Organometallic Chemistry Through the Combined Use of 2D HETCOR Solid-State NMR Spectroscopy

and Silsesquioxane Analogues. *Angew. Chem., Int. Ed.* **2001**, *40* (23), 4493−4496.
(108) Boncella, J. M.; Cajigal, M. L.; Abboud, K. A. Competition between π Donation and α-C−H Agostic Interactions in Complexes of the Type Tp'Ta(CH- *t* -Bu)(X)(Y) (X = Halide; Y = Halide, NR_2, OR; Tp'= Hydrotris(3,5-Dimethylpyrazolyl)Borate). *Organometallics* **1996**, *15* (7), 1905−1912.
(109) Churchill, M. R.; Youngs, W. J. Crystal Structure and Molecular Geometry of Ta(: CHCMe3)2(Mesityl)(PMe3)2, a Bis(Alkylidene) Complex of Tantalum with Remarkably Obtuse Ta: C(.Alpha.)-C(.Beta.) Angles of 154.0(6) and 168.9(6).Degree. *Inorg. Chem.* **1979**, *18* (7), 1930−1935.
(110) Stang, P. J.; Roberts, K. A. Generation and Trapping of Alkynolates from Alkynyl Tosylates: Formation of Siloxyalkynes and Ketenes. *J. Am. Chem. Soc.* **1986**, *108* (22), 7125−7127.
(111) Firl, J.; Runge, W. 13C-NMR Spectrum of Ketene. *Angew. Chem., Int. Ed. Engl.* **1973**, *12* (8), 668−669.
(112) Tidwell, T. T. Ketene Chemistry: The Second Golden Age. *Acc. Chem. Res.* **1990**, *23* (9), 273−279.
(113) Lavigne, F.; Maerten, E.; Alcaraz, G.; Branchadell, V.; Saffon-Merceron, N.; Baceiredo, A. Activation of CO2 and SO2 by Boryl(Phosphino)Carbenes. *Angew. Chem., Int. Ed.* **2012**, *51* (10), 2489−2491.
(114) Antoni, P. W.; Reitz, J.; Hansmann, M. M. N2/CO Exchange at a Vinylidene Carbon Center: Stable Alkylidene Ketenes and Alkylidene Thioketenes from 1,2,3-Triazole Derived Diazoalkenes. *J. Am. Chem. Soc.* **2021**, *143* (32), 12878−12885.
(115) Lavallo, V.; Canac, Y.; Donnadieu, B.; Schoeller, W. W.; Bertrand, G. CO Fixation to Stable Acyclic and Cyclic Alkyl Amino Carbenes: Stable Amino Ketenes with a Small HOMO-LUMO Gap. *Angew. Chem., Int. Ed.* **2006**, *45* (21), 3488−3491.
(116) Frey, J.; Rappoport, Z. Generation and Detection of a Relatively Persistent Carboxylic Acid Enol-2,2-Bis(2′,4′,6′-Triisopropylphenyl)Ethene-1,1-Diol. *J. Am. Chem. Soc.* **1996**, *118* (22), 5169−5181.
(117) Kuehn, L.; Eichhorn, A. F.; Schmidt, D.; Marder, T. B.; Radius, U. NHC-Stabilized Copper(I) Aryl Complexes and Their Transmetalation Reaction with Aryl Halides. *J. Organomet. Chem.* **2020**, *919*, 121249.
(118) Gonsales, S. A.; Ghiviriga, I.; Abboud, K. A.; Veige, A. S. Carbon Dioxide Cleavage across a Tungsten-Alkylidyne Bearing a Trianionic Pincer-Type Ligand. *Dalton Trans.* **2016**, *45* (40), 15783−15785.
(119) Krogman, J. P.; Foxman, B. M.; Thomas, C. M. Activation of CO2 by a Heterobimetallic Zr/Co Complex. *J. Am. Chem. Soc.* **2011**, *133* (37), 14582−14585.
(120) Escomel, L.; Del Rosal, I.; Maron, L.; Jeanneau, E.; Veyre, L.; Thieuleux, C.; Camp, C. Strongly Polarized Iridiumδ–Aluminumδ+-Pairs: Unconventional Reactivity Patterns Including CO2Cooperative Reductive Cleavage. *J. Am. Chem. Soc.* **2021**, *143* (12), 4844−4856.
(121) Cooper, O.; Camp, C.; Pécaut, J.; Kefalidis, C. E.; Maron, L.; Gambarelli, S.; Mazzanti, M. Multimetallic Cooperativity in Uranium-Mediated CO2 Activation. *J. Am. Chem. Soc.* **2014**, *136* (18), 6716−6723.
(122) Sinhababu, S.; Radzhabov, M. R.; Telser, J.; Mankad, N. P. Cooperative Activation of CO2 and Epoxide by a Heterobinuclear Al-Fe Complex via Radical Pair Mechanisms. *J. Am. Chem. Soc.* **2022**, *144* (7), 3210−3221.
(123) Sinhababu, S.; Lakliang, Y.; Mankad, N. P. Recent Advances in Cooperative Activation of CO2 and N2O by Bimetallic Coordination Complexes or Binuclear Reaction Pathways. *Dalton Trans.* **2022**, *51* (16), 6129−6147.
(124) Liu, H.-Y.; Schwamm, R. J.; Hill, M. S.; Mahon, M. F.; McMullin, C. L.; Rajabi, N. A. Ambiphilic Al−Cu Bonding. *Angew. Chem., Int. Ed.* **2021**, *60* (26), 14390−14393.
(125) Corona, H.; Pérez-Jiménez, M.; de la Cruz-Martínez, F.; Fernández, I.; Campos, J. Divergent CO 2 Activation by Tuning the Lewis Acid in Iron-Based Bimetallic Systems. *Angew. Chem.* **2022**, *134* (40), No. e202207581.
(126) Hicks, J.; Mansikkamäki, A.; Vasko, P.; Goicoechea, J. M.; Aldridge, S. A Nucleophilic Gold Complex. *Nat. Chem.* **2019**, *11* (3), 237−241.
(127) McManus, C.; Hicks, J.; Cui, X.; Zhao, L.; Frenking, G.; Goicoechea, J. M.; Aldridge, S. Coinage Metal Aluminyl Complexes: Probing Regiochemistry and Mechanism in the Insertion and Reduction of Carbon Dioxide. *Chem. Sci.* **2021**, *12* (40), 13458−13468.

https://doi.org/10.1021/jacs.4c02172
J. Am. Chem. Soc. 2024, 146, 18306−18319